University of Maribor
Faculty of Energy Technology

Journal of ENERGY TECHNOLOGY

Volume 16 / Issue 1
JUNE 2023
www.fe.um.si/en/jet.html

Journal of ENERGY TECHNOLOGY

VOLUME 16 / Issue 1

Revija Journal of Energy Technology (JET) je indeksirana v bazah INSPEC© in Proquest's Technology Research Database.

The Journal of Energy Technology (JET) is indexed and abstracted in database INSPEC© and Proquest's Technology Research Database.

JOURNAL OF ENERGY TECHNOLOGY

Ustanovitelj / FOUNDER

Fakulteta za energetiko, UNIVERZA V MARIBORU /
FACULTY OF ENERGY TECHNOLOGY, UNIVERSITY OF MARIBOR

Izdajatelj / PUBLISHER

Fakulteta za energetiko, UNIVERZA V MARIBORU /
FACULTY OF ENERGY TECHNOLOGY, UNIVERSITY OF MARIBOR

Tehnični urednik / TECHNICAL EDITOR

Sonja Novak

Tehnična podpora / TECHNICAL SUPPORT

Tamara BREČKO BOGOVČIČ

Izhajanje revije / PUBLISHING

Revija izhaja štirikrat letno v nakladi 100 izvodov. Članki so dostopni na spletni strani revije - www.fe.um.si/si/jet.html / The journal is published four times a year. Articles are available at the journal's home page - www.fe.um.si/en/jet.html.

Cena posameznega izvoda revije (brez DDV) / Price per issue (VAT not included in price): 50,00 EUR.

Informacije o naročninah / Subscription information: http://www.fe.um.si/en/jet/subscriptions.html

Lektoriranje / LANGUAGE EDITING

TAIA INT d.o.o.

Oblikovanje in tisk / DESIGN AND PRINT

Tiskarna Saje d.o.o.

Naslovna fotografija / COVER PHOTOGRAPH

Jurij AVSEC

Oblikovanje znaka revije / JOURNAL AND LOGO DESIGN

Andrej PREDIN

Ustanovni urednik / FOUNDING EDITOR

Andrej PREDIN

Izdajanje revije JET finančno podpira Javna agencija za raziskovalno dejavnost Republike Slovenije iz sredstev državnega proračuna iz naslova razpisa za sofinanciranje domačih znanstvenih periodičnih publikacij / The Journal of Energy Technology is co-financed by the Slovenian Research Agency.

Spoštovani bralci revije Journal of energy technology (JET)

Zgodovina uporabe matematike sega vsaj nekaj deset tisoč let v zgodovino. Tako so na primer v zgornjem toku Nila našli približno 20.000 let staro kost, na kateri se vidijo zareze, ki naj bi pomenile neko vrsto štetja oz. evidence. Obstajajo tudi risbe, ki so veliko starejše od prvih pismenih zapisov in nakazujejo na znanje o matematiki in merjenju časa na podlagi navideznih leg zvezd na nočnem nebu. S pojavom pisnih besedil se je na raznolikih mestih tekom zgodovine ohranilo kar nekaj zapisov o uporabi matematike – že v starem Egiptu sta bili matematika in njena uporaba na relativno visokem nivoju. To znanje so Egipčani uporabljali pri vsakodnevnih opravilih, astronomiji, … Matematika kot znanstvena veda se tudi danes naglo razvija v vseh svojih smereh in sočasno z njenim razvojem se širi tudi uporaba matematike v energetiki. V povezavi z razvojem računalniških zmogljivosti ter razvojem matematike in energetike je uporaba matematike za reševanje energetskih problemov vse pomembnejša. Tako je tudi v tej številki predstavljenih kar nekaj člankov, ki vključujejo zanimivo uporabo matematike, še posebej pa izstopa članek, v katerem je predstavljena uporaba mehke logike.

Ob izidu prve številke v šestnajsti izdaji želim vsem bralcem zanimivo in prijetno branje.

Jurij AVSEC
odgovorni urednik revije JET

Dear Readers of the Journal of Energy Technology (JET)

The history of the use of mathematics goes back at least several tens of thousands of years. For example, a bone about 20,000 years old was found in the upper reaches of the Nile. You can see notches on it, which may indicate some kind of counting or recordkeeping. There are also drawings dating back to a time long before written records that suggest a knowledge of mathematics and timekeeping based on the apparent positions of the stars in the night sky. With the advent of written texts, quite a few records of the use of mathematics have been preserved in various places throughout history. In ancient Egypt, mathematics and its application was already at a relatively high level. The Egyptians used the knowledge of mathematics in everyday tasks, as well as for astronomy, etc. Mathematics, as a science, is witnessing significant development even today, branching out in multiple directions. Alongside this development in mathematics is its use in energy technologies. In connection with the development of computing capabilities, the development in mathematics and energy and the application of mathematics in solving energy problems is becoming even more important. Even in the presented issue, there are quite a few articles that include an interesting use of mathematics. The article that highlights the use of soft logic stands out in particular.

With the release of the first issue in its sixteenth edition, I hope our readers find their reading experience engaging and enjoyable.

Jurij AVSEC
Editor-in-chief of JET

Table of Contents
Kazalo

Journal of Energy Technology

JET Volume 16 (2023) p.p. 11-22
Issue 1, 2023
Type of article: 1.01
http://www.fe.um.si/si/jet.htm

THE IMPACT OF PLUG-IN HYBRID VEHICLES IN LOW-VOLTAGE DISTRIBUTION SYSTEMS USING A MONTE CARLO SIMULATION

VPLIV PRIKLJUČNIH HIBRIDNIH VOZIL NA NIZKONAPETOSTNE DISTRIBUCIJSKE SISTEME Z UPORABO METODE MONTE CARLO

Evica Smilkoska[1], Vasko Zdraveski, Jovica Vuletić, Jordančo Angelov, Mirko Todorovski[2]

Keywords: Plug-in Hybrid Electric Vehicle, Power Quality, Non-Deterministic Approach, Voltage Deviations, Power Losses, Distribution Systems.

Abstract

The growing presence and randomness of renewable-based Distributed Generation, such as solar, photovoltaic, and wind power, and heavy Plug-in Hybrid Electric Vehicle loads in residential distribution grids result in both a higher degree of imbalance and a wide range of voltage fluctuations. When increasing the number of Plug-in Hybrid Electric Vehicles that are simultaneously charged, the additional unpredicted load may cause several problems to the current grid in terms of voltage deviations, thermal overloads, power losses, increased aging of transformers and lines, decreased quality of supply, and power outages. This paper proposes an approach that models Plug-in Hybrid Electric Vehicles' behaviour and performs power flow analysis on CIGRE low voltage benchmark grid to investigate the impact on the current distribution grid.

1 Evica Smilkoska, Elektrodistribucija DOOEL, Customer Center (KEC) Gostivar, Str. Goce Delchev no.45 Gostivar, R. N. Macedonia, E-mail: evica.smilkoska@evn.mk

2 Ss. Cyril and Methodius University, Faculty of Electrical Engineering and Information Technologies, Rugjer Boskovic 18, Skopje, R. N. Macedonia, E-mails: vaskoz@pees-feit.edu.mk, jovicav@pees-feit.ukim.edu.mk, jordanco@pees-feit.edu.mk, mirko@pees-feit.edu.mk

Povzetek

Vse večja prisotnost proizvodnje, ki temelji na obnovljivih virih energije, kot je sončna, fotovoltaična in vetrna energija, njena naključna porazdeljenost ter velike obremenitve priključnih hibridnih električnih vozil (EV) v stanovanjskih distribucijskih omrežjih povzročajo tako višjo stopnjo neravnovesja kot širok razpon nihanj napetosti. S povečanjem števila priključnih hibridnih EV, ki se sočasno polnijo, lahko dodatna nepredvidljiva obremenitev povzroči več težav trenutnemu omrežju – to so odstopanja napetosti, toplotne preobremenitve, izguba moči, hitrejše staranje transformatorjev in vodov ter zmanjšana kakovost oskrbe in izpad električne energije. V članku predlagamo pristop, ki modelira obnašanje priključnih hibridnih električnih vozil in izvaja analizo pretoka moči na nizkonapetostnem referenčnem omrežju CIGRE ter na ta način omogoča raziskavo vplivov EV na trenutno distribucijsko omrežje.

1 INTRODUCTION

Distribution System Operators (DSOs) are responsible for operating their grid to follow a predicted demand with unidirectional power flows only. Most of the conventional distribution grids are of the radial type with different configurations and loads. They have one objective: to offer a quality of supply under certain technical and economic parameters that offer efficient and reliable grid operation. *[1]-[2]* Due to the fast development of power electronic technologies, the presence of Distributed Generation (DG) and connected Plug-in Hybrid Electric Vehicles (PHEVs), the bi/multi-directional power flow distribution grid is growing rapidly, which raises the question: Are the current conventional distribution grids ready for these new rapidly-growing types of loads? *[3]*
The advancements in transportation electrification have changed the structure of traditional car manufacturing processes. This kind of rapid and increased development in the transportation electrification sector requires large-scale research and evaluation in order to measure the capability of the current conventional distribution systems to withstand the increased presence of PHEVs. *[4]*

PHEVs are continuously opening up new perspectives and numerous possibilities. *[5]* These types of vehicles currently present on the market not only reduce pollution, but can also help in conserving natural resources. PHEV technology is one of the most promising forms of technology for reducing petroleum consumption associated with reducing the use of internal combustion engine vehicles, and they are seen as an opportunity to provide environmentally-friendly vehicles for transportation that do not release greenhouse gases into the atmosphere or cause smog. From an energy policy point of view, electro-mobility offers the opportunity to achieve the objectives of decarbonisation and decentralisation of electricity sources. *[6]*

As one of the types of Electric Vehicles (EVs), PHEVs are recharged through a plug connected to the electric power grid. *[4]* Hence, PHEVs are changing the conventional load profile. *[7]-[8]* The main issues caused by their growing presence are mainly related to power quality. Power quality is a predominant aspect of the efficiency and security of grids and is likely to be strongly affected by PHEV development over the forthcoming years. *[9]*

'Power Quality' refers to providing a near sinusoidal voltage and current waveforms for the power grid at the rated magnitude and frequency. *[10]* Factors such as voltage and frequency variations, imbalance, interruption, flicker, and harmonics can determine power quality. As the number of PHEVs that are randomly charged on the grid is increasing rapidly, the unpredicted load profile

may pose several problems to the current conventional grid in terms of voltage deviations, thermal overloads, power losses, increased aging of transformers and lines, decreased quality of supply and power outages. It is thus of great importance to investigate power quality concerns in distribution grids when considering PHEVs.

The impact of PHEVs on the grid's parameters can be consequential or inconsequential depending on the number of PHEVs attached to the grid, the grid's characteristics, and the PHEV's charging features. To conclude that supplied energy is of acceptable quality, the parameters that define it must be within limits defined by the DSO distribution regulation. *[11]*

With the increased presence of PHEVs, and moving beyond the aforementioned problems associated with the quality of the distributed electric energy, the problem relating to the increased aging of transformers and lines is also significant. The solution to this problem is mainly focused on grid reinforcement. Researchers studying this problem have concluded that a large economic investment will be needed for the proposed solution. Different studies have proposed strategies as an economical alternative to grid reinforcement. *[1]* One of the proposed strategies involves PHEV charging schemes as an alternative for supporting the grid and enhancing both the efficiency and the reliability of the distribution grid. Numerous research studies show that intelligent integration, namely smart PHEV charging, can lower the impact on the power grid or provide different ancillary services. *[12]* The ancillary services provided by PHEVs are associated with the mode of discharging their batteries, i.e. discharging the stored energy for peak power shaving and spinning reserves. *[13]* On the other hand, the available energy stored in PHEVs can relieve the distribution grid from overloading at certain times or allow the grid to charge more PHEVs at any time of the day, including during peak hours. Introducing storage devices like PHEVs may result in revolutionary changes to the distribution grid, *[14]* such as voltage support, providing backup power in case of interruption, reducing losses, and postponing the need for distribution grid reinforcements.

The way the distribution grid is connected and operated to provide power to a load that changes every minute requires a time analysis to see the effect on the grid, especially with changing household loading and the timing of PHEVs cycles of charging and discharging or, in other words, demand response. *[15]* The main purpose of this paper is to analyse a specific grid configuration where feeders, conductors, transformers and substations, DGs, and PHEVs perform well while simultaneously maintaining a radial configuration and the desired supply quality. *[16]*

2 PROBLEM FORMULATION

The problem of connecting the injections generated by PHEVs in the distribution grid for 24-hour analysed intervals and analysing the power quality parameters is defined in this section using MATLAB functions.

The PHEV types used in this simulation are defined in Table 1. *[8]* There are four different groups of PHEVs, with each group containing three different PHEVs according to their All-Electric Range (AER). The AER is defined as the possible distance driven by a PHEV with a fully charged battery. *[4]* Table 1 also shows the battery capacity of PHEVs with an AER of 48, 64, and 96 km, respectively. The data shows that a PHEV's battery capacity can vary from 7.78 kWh to 27.44 kWh.

In order to precisely define the PHEVs referred to in this paper, the battery's State of Charge (SOC) has to be determined as one of the required parameters. SOC is a calculation estimate

that gives a rough estimate of the state of energy in the battery pack. *[4]* This paper defines the battery SOC as a random value between 0.3 and 0.9 of the battery capacity. These values reflect the minimum energy that must be stored in the PHEV's battery and the maximum energy up to which the PHEV's battery can be charged.

Table 1: *PHEVs battery capacity data*

Vehicle type	**PHEV$_{48}$[kWh]**	**PHEV$_{64}$[kWh]**	**PHEV$_{96}$[kWh]**
Compact sedan	7.78	10.34	15.51
Mid-size sedan	8.95	11.93	17.89
Mid-size SUV	11.33	15.11	22.67
Full-size SUV	13.72	18.29	27.44

$$\Delta SOC = 0.9 - 0.3 = 0.6 \tag{2.1}$$

$$A = rand[0,1] \tag{2.2}$$

$$\Delta SOC' = A \cdot \Delta SOC + 0.3 \tag{2.3}$$

If the battery SOC of the PHEV is < 0.5, the vehicle attached to the grid has be charged or, in other words, take energy from the grid. Conversely, if the battery SOC is > 0.5 and < 0.9, then the vehicle must discharge or inject energy into the grid.

$$PHEV = \begin{cases} \text{charging:} & SOC < 0.5 \\ \text{discharging:} & 0.5 < SOC < 0.9 \end{cases} \tag{2.4}$$

The following parameters defining the PHEVs are the arrival and departure times of PHEVs. The arrival and departure times determine their availability during the 24-hour analysed interval. The arrival time and departure time of the PHEVs have been randomly chosen from real-life databases. *[17]* Suppose the value of the departure time is lower than that of the arrival time. In this case, the departure time of the vehicle is considered to be within the next day, which falls outside of the analysed interval. The departure time is thus rounded up to midnight or the last hour of the analysed interval. After determining the needed parameters, we can generate the injection of the PHEVs during the 24-hour analysed interval.

$$ATime = rand[DataBase] \tag{2.5}$$

$$DTime = rand[DataBase] \tag{2.6}$$

$$DataBase = 01{:}00{,}02{:}00{,}\ldots.24{:}00 \tag{2.7}$$

$$DTime = \begin{cases} DTime; DTime > ATime \\ 24{:}00; DTime < ATime \end{cases} \tag{2.8}$$

In terms of the grid load, the paper uses real-life data from the site *Elektrodistribucija DOOEL. [18]* The loading data applies to households with and without electric heating during 2021. Annual data for the scale of 24-hour distribution has been extracted for this simulation. Figure 1 presents a daily diagram of the households loading with electric heating and without electric heating, respectively, during 24 hours with its minimum, maximum, and mean values according to the legends shown on the diagrams.

Based on the analysis, the load curves connected to the grid nodes are randomly selected between the highest and lowest values from the load profile curve area shown in Figure 1. Considering all of the uncertain variables in this paper, a Monte Carlo simulation is used to solve the power flow analysis in each iteration. A new loading curve is generated for every grid node, and the methodology is repeated for every iteration.

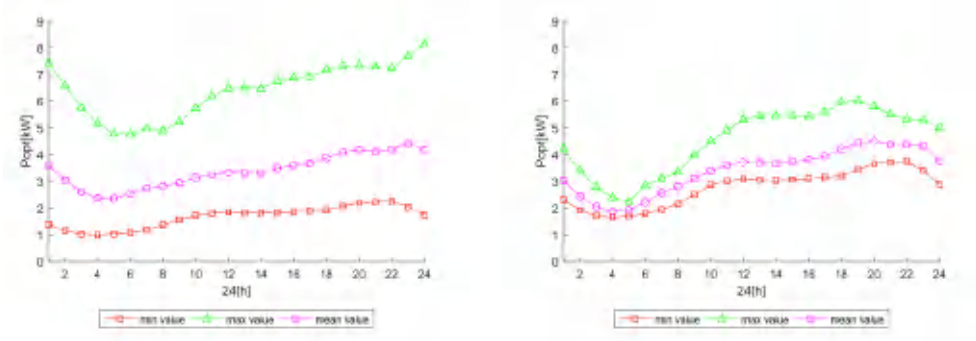

Figure 1: *Domain of the household loading curves – left with electric heating (Case One) and right without electric heating (Case Two)*

- Case 1: Household with electric heating

$$P_{value,h_i,case1} = rand[P_{min\ value,h_i,case1}, P_{max\ value,h_i,case1}] \quad (2.9)$$

$$h_i = 1,2,3\ldots24 \quad (2.10)$$

- Case 2: Household without electric heating

$$P_{value,h_i,case2} = rand[P_{min\ value,h_i,case2}, P_{max\ value,h_i,case2}] \quad (2.11)$$

$$h_i = 1,2,3\ldots24 \quad (2.12)$$

The characteristic values that determine the loading data are presented in Table 2. It can be noticed that the loading values attached to the grid are within the interval of 0.9914 kW to 8.1298 kW for households with electric heating. While again, for households without electric heating, the loading values attached to the grid are within the interval of 1.6492 kW to 6.0206 kW.

In this paper, in order to analyse the injection of PHEVs into the distribution grid and the characteristics that define the power quality, the CIGRE benchmark low voltage grid is used. *[20]* The grid's topology is presented in Figure 2, with household loads connected to every grid node.

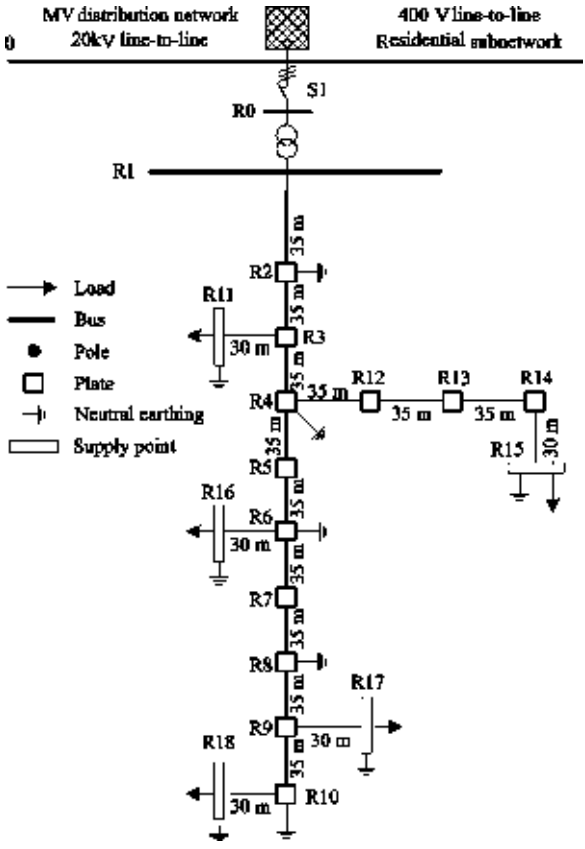

***Figure 2: CIGRE** Benchmark low voltage grid*

***Table 2:** Household loading data*

h_{no}	With electric heating			Without electric heating		
	min [kW]	max [kW]	mean [kW]	min [kW]	max [kW]	mean [kW]
1	1.3883	7.4191	3.6039	2.3096	4.2115	3.0264
2	1.1536	6.5703	3.0390	1.9192	3.3929	2.4341
3	1.0278	5.7731	2.6180	1.7099	2.7751	2.0563
4	0.9914	5.1797	2.3705	1.6492	2.3962	1.8760
5	1.0332	4.7751	2.3439	1.6969	2.2351	1.9304
6	1.0819	4.7651	2.5352	1.7812	2.8479	2.2125
7	1.1811	4.9939	2.7336	1.9385	3.0982	2.5695
8	1.3583	4.8876	2.8093	2.1587	3.3362	2.8082
9	1.5612	5.2129	2.9471	2.5006	3.9948	3.1012
10	1.7215	5.7407	3.1316	2.8639	4.4958	3.3943
11	1.8143	6.2004	3.2678	3.0182	4.9054	3.6079

12	1.8520	6.4862	3.3325	3.0810	5.3181	3.7169
13	1.8315	6.5069	3.3030	3.0469	5.4679	3.6963
14	1.8228	6.4792	3.3098	3.0324	5.4789	3.6669
15	1.8376	6.7738	3.4915	3.0571	5.4663	3.7338
16	1.8596	6.8856	3.5979	3.0936	5.4246	3.8048
17	1.8909	6.9139	3.6771	3.1458	5.5919	3.9519
18	1.9282	7.1817	3.8842	3.2078	5.9616	4.2007
19	2.0656	7.3305	4.0904	3.4363	6.0206	4.4399
20	2.2005	7.3505	4.1649	3.6608	5.8126	4.5026
21	2.2284	7.3101	4.1181	3.7072	5.5252	4.3869
22	2.2481	7.2631	4.1809	3.7400	5.3398	4.3885
23	2.0472	7.6929	4.4291	3.4057	5.2919	4.3145
24	1.7388	8.1298	4.1697	2.8927	5.0012	3.7669

The Power Flow analysis of the low-voltage distribution grid is made using a suitable mathematical model. *[21]* The Power Flow analysis determines the power distribution in the grid branches and voltages in the grid's nodes.

3 CASE STUDY

The case study consists of two different case studies depending on the loading attached to the grid. Case One consists of loading data with electric heating, while Case Two consists of loading data without electric heating. The simulation for each case is performed once when there are PHEVs injections attached to the distribution grid and once when there are no PHEVs injections attached to the distribution grid in order to compare the results between the two Cases for the branch's active power loss and node voltage drop. For every node of the CIGRE Benchmark low voltage distribution grid, a new injection for the 24-hour analysed interval from one randomly chosen PHEV is created, and a new curve for the loading profile is generated depending on the analysed case. Since the grid has 18 nodes, 17 new PHEV injections are generated, 17 different loading profiles are generated, and one power flow analysis is performed. Node R1 does not form part of the analysis. The result from one iteration is a 24-hour probability distribution (PD) for the branch's active power loss and the node's voltage drop interval.

The simulation for Case One with PHEV injections attached to the distribution grid and Case One without PHEV injections attached to the distribution grid is performed 10,000 times to provide detailed information regarding the PD of the branch's active power losses and the node voltage magnitudes. The same procedure is then repeated for Case Two.

As mentioned earlier, this paper considers the Monte Carlo method for solving the power flow simulation. The values subject to analysis are randomly sampled during a Monte Carlo simulation. Each set of samples is called an iteration, and the resulting outcome from each sample is recorded. Here, the results recorded are the branch active power losses and node voltages. With the Monte Carlo simulation performed hundreds or thousands of times, the result is a probability distribution of possible outcome values of the branch active power losses and node voltages. As a result, the Monte Carlo simulation provides a much more comprehensive view of what may happen.

The desired output of the power flow analysis is the domain of the active power losses in the grid, presented by its min, max, and mean values, and the domain of the voltages in the nodes, respectively. It is expected that when the active power loss value in the grid is maximum, the node voltages values are minimum due to high values of the loading.

The comprehensive presentation of the generated PHEV injections represented by their minimum, maximum, and mean values is presented in Figure 3.

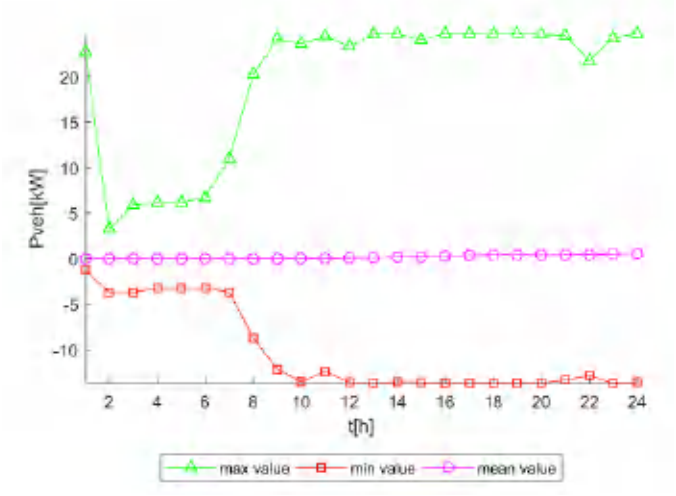

Figure 3: *Domain of the generated PHEVs injections*

From the presented data of the generated injections, we note that the domain of the PHEVs attached to the grid is between 24.6939 kW and -13.7191 kW. The results for active power losses and node voltages for Case One after the simulation are presented in Figure 4 and Figure 5, respectively.

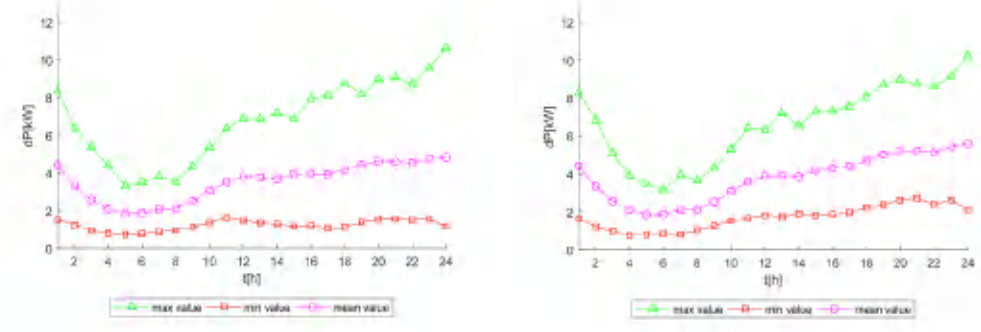

Figure 4: *Active power losses - left without PHEVs, right with PHEVs – Case One (with electric heating)*

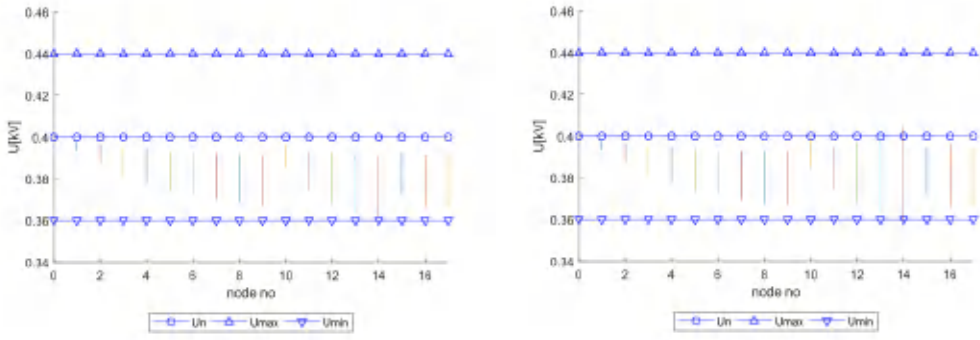

Figure 5: *Histogram of node voltages - left without PHEVs, right with PHEVs – Case One (with electric heating)*

Next is the simulation for Case Two. The results for active power losses and node voltages for Case Two are presented in Figure 6 and Figure 7, respectively.

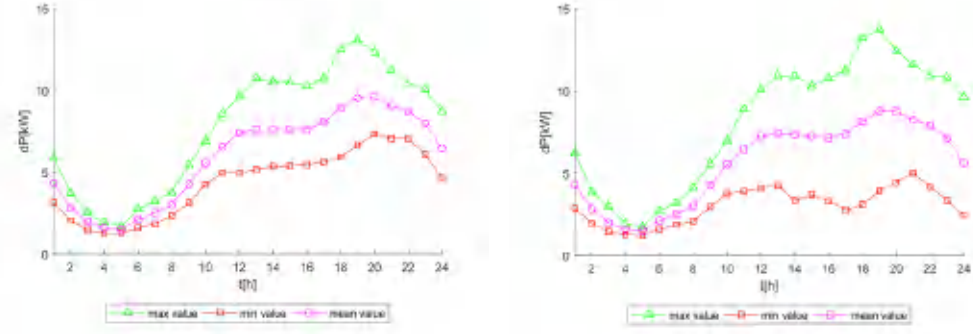

Figure 6: *Active power losses - left without PHEVs, right with PHEVs – Case Two (without electric heating)*

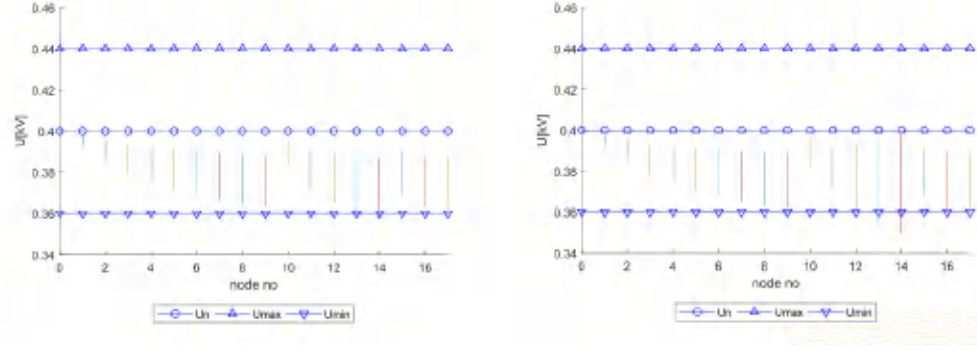

Figure 7: *Histogram of node voltages - left without PHEVs, right with PHEVs – Case Two (without electric heating)*

From the presented results for Case One, the domain of the grid active power losses with and without PHEVs is mainly overlapped. The domain of the active power losses consists of larger values when no PHEVs are connected to the grid, which is unlike when PHEVs are connected to the grid, as confirmed by the presented results. When we analyse the scenario without PHEVs, the curves of the active power losses generally follow the curve of the loading profile, something which is not the case when we analyse the scenario with connected PHEVs. In such cases, the active power losses curve follows the same trend but with certain peak shaving, depending on the PHEVs injections. As for the results of the node voltages for Case One and the given constraints, almost all are beneath the nominal grid voltage (0.4 kV). However, besides this, all of the values are in the DSOs given constraints of ΔU = ± 10%, with and without connected PHEVs, respectively. From the presented results, we note a deviation of voltage magnitudes, which is more significant when PHEVs are connected to the grid and somewhat smaller when PHEVs are absent. When PHEVs are connected, the distribution grid performs well while maintaining both a radial configuration and the desired supply quality as defined by the DSO distribution regulation. Unlike Case One, Case Two is characterised by a different domain of the household loading curves, which means that the domain of the grid active power losses with and without PHEVs will differ. The domain of the active power losses in Case Two consists of slightly larger values than in Case One. According to the presented results, it is characterised by the same diversity both when PHEVs are connected to the grid and when PHEVs are absent. As for the results of the node voltages for Case Two, a difference in voltage magnitudes is noted from the presented results. When PHEVs are absent, the voltage magnitudes are lower the nominal grid voltage (0.4 kV), but nevertheless fulfil the DSO's given constraints of ΔU = ± 10%. This is not the case when PHEVs are connected to the grid. In this case, one node, Node No 14, did not fulfil the DSOs given constraints ΔU = ± 10%. All the other voltage magnitudes are beneath the nominal grid voltage (0.4 kV). In this case, the households connected to that node will face a slight malfunction resulting in lowered power quality determined by several factors, such as voltage and frequency variations, imbalance, interruption, and flicker.

4 CONCLUSION

The increasing presence of PHEVs in daily life is inevitable. Their presence in the years that follow will increase exponentially. According to the presented results, PHEVs will impact the current distribution grid. These impacts can be significant or insignificant, depending on the number of PHEVs attached to the grid, grid characteristics, and PHEV charging features. This is despite the negative impact of PHEVs' charging/discharging cycles on battery life.

Technical and economic factors must also be considered when reducing the impact of PHEVs on the distribution grid. The proposed methods align with integrating new charging schemes and coordinating their charging and discharging cycles. *[22]* With the smart charging of PHEVs, the peak from charging PHEVs will be shifted to periods with a lower peak from the household loading. The characteristic of PHEV for bi/multi-directional power flow can be used as a strategy for regulating the grid voltage. The active power control can also adjust the operation of PHEV charging, while the reactive power control can inject reactive power into the grid to support the network voltage. The proposed methods should be the subject of further research.

References

[1] **S. Martinenas, K. Knezović, M. Marinelli:** *Management of Power Quality Issues in Low Voltage Networks using Electric Vehicles: Experimental Validation*, IEEE Transactions on Power Delivery, Volume: 32 Issue: 2, 2016

[2] **M. M. Biswas, S. R. Akhter, K. C. Paul:** *Power Quality Analysis for Distributed Generation and Electric Vehicle Integrated Distribution System*, IEEE 2020 55th International Universities Power Engineering Conference (UPEC), Torino, Italy, 2020

[3] **T. Aljohani, O. Mohammed:** *Modeling the Impact of the Vehicle-to Grid Services on the Hourly Operation of the Power Distribution Grid*, Energy System Research Laboratory, Florida International University, Miami, Florida, 2018

[4] **P.-Y. Kong, G. K. Karagiannidis**: *Charging Schemes for Plug-In Hybrid Electric Vehicles in Smart Grid: A Survey*, IEEE Access (Volume: 4), pp. 6846 – 6875, 2016

[5] **Z. Darabi, M. Ferdowsi:** *Plug-in Hybrid Electric Vehicles: Charging Load Profile Extraction Based on Transportation Data*, 2011 IEEE Power and Energy Society General Meeting, 2011

[6] **J. Baraniak, J. Starzynski:** *Modeling the Impact of Electric Vehicle Charging Systems on Electric Power Quality*, Article, Energies 2020

[7] **S. Shao, M. Pipattanasomporn, S. Rahman**: *Challenges of PHEV Penetration to the Residential Distribution Network*, 2009 IEEE Power & Energy Society General Meeting, Calgary, Alberta Canada, 2009

[8] **V. Zdraveski, P. Krstevski, J. Vuletic, J. Angelov, A. Krkoleva Mateska, M. Todorovski:** *Analyzing the Impact of Battery Electric Vehicles on Distribution Networks Using Non-deterministic Model*, IEEE EUROCON 2019 -18th International Conference on Smart Technologies, Novi Sad, Serbia, 2019

[9] **M. Sabarimuthu, N. Senthilnathan, A. M. Monnisha, V. Kamalesh Kumar, S. KrithikaSree, P.Mala Sundari:** *Measurement and Analysis of Power Quality Issues Due to Electric Vehicle Charger*, IOP Conference Series Materials Science and Engineering, 2021

[10] **A. Ahmadi, A. Tavakoli, P. Jamborsalamati, N. Rezaei, M. Reza Miveh, F. Heidari Gandoman, A. Heidari, A. Esmaeel Nezhad:** *Power quality improvement in smart grids using electric vehicles: a review*, IET Electrical Systems in Transportation, Volume 9, Issue 2, pp. 53-64, 2019

[11] **Energy Regulatory Commission**: *Electricity Distribution Network Rules*, Energy Regulatory Commission Official page, 2019

[12] **S. Shao, M. Pipattanasomporn, S. Rahman**: *Challenges of PHEV Penetration to the Residential Distribution Network*, 2009 IEEE Power & Energy Society General Meeting, Calgary, Alberta Canada, 2009

[13] **F. Li, L. Guo, L. Liu, X. Li, Q. Wang**: *Method to improve charging power quality of electric vehicles*, The 14th IET International Conference on AC and DC Power Transmission (ACDC 2018), The Journal of Engineering, Chengdu, China, 2018

[14] **B. Zargar, T. Wang, M. Pitz, R. Bachmann, M. Maschmann, A. Bintoudi, L. Zyglakis, F. Ponci, A. Monti, D. Ioannidis:** *Power Quality Improvement in Distribution Grids via Real-Time Smart Exploitation of Electric Vehicles*, Article, Energies, 2021

[15] **T. Aljohani, O. Mohammed:** *Modeling the Impact of the Vehicle-to Grid Services on the Hourly Operation of the Power Distribution Grid*, Energy System Research Laboratory, Florida International University, Miami, Florida, 2018

[16] **E. O. Santos, J. S. B. Martins**: *Distribution Power Network Reconfiguration in the Smart Grid*, CIGRÉ-BRASIL - Brazilian National Committee, International Seminar on Policies, Incentives, Technology and Regulation on Smart Grids, Rio de Janeiro, Brasil, 2017

[17] **National Highway Traffic Safety Administration:** https://www.nhtsa.gov/, date of access March 2022

[18] **Elektrodistribucija DOOEL – Standard annual load distribution curve 2021:** https://www.elektrodistribucija.mk/, date of access March 2022

[19] **J. Angelov, J. Vuletik, M. Todorovski:** *Optimal Locations of Energy Storage Devices in Low-Voltage Grids*, ICEST 2019, Ohrid, Macedonia, 2019

[20] *Benchmark systems for network integration of renewable and distributed energy resources*, Cigre Task Force C6.04.02, Tech. Rep, 2014

[21] **F. Dilsiz**: *Power Flow Analysis - Power Flow Study*, the International University of Sarajevo, Faculty of Engineering and Natural Sciences, 2014

[22] **L. Hui-ling, B. Xiao-min, T. Wen**: *Impacts of Plug-in Hybrid Electric Vehicles Charging on Distribution Grid and Smart Charging*, 2012 IEEE International Conference on Power System Technology (POWERCON), Auckland. New Zealand, 2012

Nomenclature

ΔSOC	domain of the PHEVs state of charge
A	A random value between 0 and 1
$\Delta SOC'$	State of Charge assigned to the PHEV
$ATime_{veh}$	random value for the arrival time of the PHEV from the Data Base
$DTime_{veh}$	random value for the departure time of the PHEV from the Data Base
Data Base	Data Base with values for arrival and departure time for the PHEVs
$P_{value,\ hi,case1}$	value for the load in each hour randomly chosen between the min and the max values of the load profile curve area for Case One
$P_{value,\ hi,case2}$	value for the load in each hour randomly chosen between the min and the max values of the load profile curve area for Case Two
h_i	each hour of the analysed interval

JET Journal of Energy Technology

JET Volume 16 (2023) p.p. 23-40
Issue 1, 2023
Type of article: 1.01
http://www.fe.um.si/si/jet.htm

GENERALISED FUZZY LINEAR PROGRAMMING

GENERALIZIRANO MEHKO LINEARNO PROGRAMIRANJE

Janez Usenik*, Maja Žulj[1]

Keywords: linear programming, fuzzy linear programming, generalised linear programming, generalised fuzzy linear programming

Abstract

Linear programming is one of the widely used methods for optimising business systems, which includes organisational, financial, logistic and control subsystems of energy systems in general. It is possible to express numerous real-world problems in a form of linear program and then solve by simplex method *[1]*. In the development of linear programming, we are facing a number of upgrades and generalisations, as well as replenishment. Particularly interesting in recent years is an option that decision variables and coefficients are fuzzy numbers. In this case we are dealing with fuzzy linear programming. If we also include in a fuzzy linear program a generalisation with respect to Wolfe's modified simplex method *[1],* we obtain a generalised fuzzy linear program (GFLP). Usenik and Žulj introduced methods for solving those programs and proved the existence of the optimal solution in *[2].* In the article, the simplex algorithm which enables the determining of an optimal solution for GFLP is described. There is a numerical example at the end of the article that illustrates the algorithm.

Povzetek

Linearno programiranje je najbolj uporabljena metoda optimizacije poslovnih sistemov, med katere štejemo tudi organizacijske, finančne, logistične in nasploh upravljalne podsisteme energetskega sistema. Veliko praktičnih problemov je mogoče izraziti v obliki linearnega programa, ki ga nato rešimo s simpleksno metodo *[1].* Razvoj linearnega programiranja je doživel vrsto nadgradenj, posplošitev in dopolnitev. V zadnjih letih je še posebej zanimiva možnost, da so odločitvene spremenljivke in koeficienti mehka števila – v tem primeru gre za mehko linearno programiranje. Ko pa v ta program uvedemo še pojem generalizacije v Wolfejev pomenu *[1]*, govorimo o generaliziranem mehkem linearnem programiranju (GMLP). Usenik in Žulj *[2]* sta razvila postopke reševanja takšnih programov in dokazala eksistenco optimalne rešitve. V članku opišemo algoritem simpleksnega postopka za GMLP, ki omogoča izračun optimalne rešitve, in na koncu dodamo numerični primer, ki ilustrira izvedeni algoritem.

* Corresponding author: Prof. Janez Usenik, PhD, Tel.: +38640 647 686, E-mail address: janez.usenik@guest.um.si

1 University of Maribor, Faculty of Energy Technology, Hočevarjev trg 1, 8270 Krško, Slovenia, E-mail address: maja.zulj@um.si

1 INTRODUCTION

Linear programming is one of the most frequently used techniques in operations research, introduced in 1939 by Russian mathematician Leonid Vitalijevič Kantorovič, who also proposed a method for solving it. Between 1946 and 1947, American mathematician Georg Bernard Dantzig defined a general formulation of linear programming. In 1947, he introduced the so-called simplex method, a method that enables the successful solving of any linear programming problem [1]. Linear programming can be used in economic science and in the management of business or organisational systems, as well as in actions like production planning, the optimisation of the technological process, an optimal logistics service, optimal outsourcing, etc. Linear programming proved to be of considerable applicative importance at the time computers became more capable. Nowadays, a variety of competent computer software programs exist that even enable problems of enormous dimensions to be easily solved.

The theory of linear programming is developing in different ways. Let us point out two alternatives in this field. In the first alternative we use a dynamic approach, where we study the optimal behaviour of variables, which are functions of time in this approach. This problem is called continuous variable dynamic linear programming *[3], [4].* In *[5]* we can find a generalisation of c/b/A-continuous variable dynamic linear programming in the sense of Wolfe generalisation *[1].*

This generalisation is based on the condition that elements of some columns of matrix $A(t)$, at the time of formulating the problem, are unknown, but linked convexly in columns. In this case, we talk about *generalised continuous variable dynamic linear programming.*

The second alternative, which has attracted a lot of interest, especially in the last 20 years, is linear programming in conditions represented by fuzzy logic. In this matter, we are dealing with *fuzzy linear programming.* It is a tool for modelling imprecise data and it is based on fuzzy sets *[6].* In 1978, Zimmermann proposed the formulation of fuzzy linear programming problems in [7]. Since then, researchers have developed a relatively large number of different methods to solve such problems. It also turns out that there are no obstacles for generalisation in fuzzy linear programming. In this case, we talk about *generalised fuzzy linear programming.* Usenik and Žulj introduced methods for solving those programs and proved the existence of the optimal solution in *[2].*

2 FUZZY LINEAR PROGRAMMING

2.1 Fuzzy numbers

A fuzzy number is a generalisation of a regular real number in the sense that it does not refer to one single value but rather to a connected set of possible values. It is a special case of fuzzy sets, which were introduced by Lotfi A. Zadeh in *[6].* A fuzzy set $\tilde{A}$ is a set of ordered pairs: $\tilde{A}=\left\{\left(x,\mu_{\tilde{A}}(x)\right)\middle| x\in R\right\}$ where $\mu_{\tilde{A}}(x)$ is the membership function of x, which maps R to a subset of the non-negative real numbers whose supremum is finite. If $\sup_x \mu_{\tilde{A}}(x)=1$, the fuzzy set $\tilde{A}$ is called normal and if $\mu_{\tilde{A}}\left(tx+(1-t)y\right)\geq \min\left\{\mu_{\tilde{A}}(x),\mu_{\tilde{A}}(y)\right\}$, $x,y\in R$, $t\in[0,1]$, the fuzzy set $\tilde{A}$ is convex. Fuzzy number $\tilde{A}$ is a convex normalised fuzzy set $\tilde{A}$ on the real line, such that there exists at least one $x_0\in R$ with

$\mu_{\tilde{A}}(x_0)=1$ and where $\mu_{\tilde{A}}(x)$ is piecewise continuous, *[7]*. In the numerical example at the end of the article are triangular fuzzy numbers, represented with tree points: $\tilde{A}=(a,b,c)$, with membership function:

$$\mu_{\tilde{A}}=\begin{cases}\dfrac{1}{b-a}x-\dfrac{a}{b-a} & \text{for } a\le x\le b\\ -\dfrac{1}{c-b}x+\dfrac{c}{c-b} & \text{for } b\le x\le c\\ 0 & \text{otherwise}\end{cases}$$

Let $F(R)$ be the set of triangular fuzzy numbers, and $\tilde{A},\tilde{B}\in F(R)$ are given as $\tilde{\mathrm{A}}=(\mathrm{a}_1,\mathrm{a}_2,\mathrm{a}_3)$, $\tilde{B}=(\mathrm{b}_1,\mathrm{b}_2,\mathrm{b}_3)$, $\lambda\in R$. Then operations of triangular fuzzy numbers are defined as
$\tilde{A}+\tilde{B}=(a_1+b_1,a_2+b_2,a_3+b_3)$; $\tilde{A}-\tilde{B}=(a_1-b_3,a_2-b_2,a_3-b_1)$;
$\lambda\tilde{A}=(\lambda a_1,\lambda a_2,\lambda a_3)\quad for\quad \lambda\ge 0$ and $\lambda\tilde{A}=(\lambda a_1,\lambda a_2,\lambda a_3)\quad for\quad \lambda<0$.

The nature of simplex algorithms in linear programming problems involves comparison, or so-called ranking, of fuzzy numbers. There is no generally accepted criteria for comparison of fuzzy numbers. One convenient method for comparison is the method of ranking functions. Ranking function $\mathbf{R}:F(R)\to R$ is a mapping from the set of fuzzy quantities into the set of real numbers. Fuzzy numbers can then be compared according to the corresponding real numbers. Several number-ranking functions can be found in the literature. For ranking triangular fuzzy numbers in the numerical example at the end of this article, the Chens method *[8]* is used.

2.2 Fuzzy linear programming

A general model of a linear programming problem can be written as:

$$\begin{aligned}&\text{maximize} && cx\\ &\text{subject to} && Ax\le b\\ & && x\ge 0\end{aligned}\qquad (2.1)$$

If some of the coefficients (c,A,b) in a linear program (2.1) cannot be precisely defined, we can treat them as fuzzy numbers and call this linear program a fuzzy linear program. Based on the place where fuzzy numbers appear, we can divide fuzzy linear programming (FLP) problems into four main categories:

- FLP with fuzzy resources ($\tilde{b}$);
- FLP with fuzzy coefficients in an objective function ($\tilde{c}$);
- FLP with fuzzy technological coefficients ($\tilde{a}_{ij}$);
- FLP with fuzzy variables ($\tilde{x}$).

By combining these four categories, we obtain many different types of fuzzy linear programming problems, each of them solvable using a different method. Around 50 methods have been analysed and a basis for a taxonomy of different methods has been published in *[9]*.

The fuzzy linear program for $c\in R^n,\tilde{x}\in\left[F(R)\right]^n,\tilde{b}\in\left[F(R)\right]^m,A\in R^{m\times n}$ is in canonical form (completed with slack and artificial variables), defined by expressions:

$$\begin{aligned} opt\ \ & \tilde{z} = (c, \tilde{x}) \\ \text{subject to}\ \ & A\tilde{x} = \tilde{b} \\ & \tilde{x} \geq 0 \end{aligned} \tag{2.2}$$

where fuzzy quantities are compared according to a selected ranking method. Fuzzy vector $\tilde{x} \in (F(R))^n$ is a feasible solution for the problem (2.2) if and only if $\tilde{x}$ satisfies the constraints of the problem. A fuzzy feasible solution $\tilde{x}_{opt}$ is a fuzzy optimal solution for problem (2.2), if for all fuzzy feasible solutions $\tilde{x}$, we have $(c, \tilde{x}_{opt}) \geq (c, \tilde{x})$ when optimum means maximum, or $(c, \tilde{x}_{opt}) \leq (c, \tilde{x})$ when optimum means minimum. There are several methods to solve fuzzy linear programs, many of them analysed in *[2].*

3 GENERALISED FUZZY LINEAR PROGRAMMING

In the article we are dealing with the generalisation of fuzzy linear programming in accordance with the Wolfe approach *[1], [3], [5]*. Therefore, we tackle the problem concerning a linear program where technological coefficients and coefficients in an objective function are not precisely known. But we know that these coefficients are integrated in some known convex composition, i.e., the limited material, financial, logistic, energy, ecological or human resource that is required to produce some product, service, or similar.

Consider the fully fuzzy linear program in standard and canonical form:

$$\begin{aligned} & opt\, z = (\tilde{c}, \tilde{x}) \\ & \tilde{A}\tilde{x} = \tilde{b} \\ & \tilde{x} \geq \tilde{0} \end{aligned} \tag{3.01}$$

where:

$\tilde{c} = (\tilde{c}_1, \tilde{c}_2, \ldots, \tilde{c}_n)$, $\tilde{c}_i \geq \tilde{0}, i = 1, 2, \ldots, n$; a vector with either all, some or no components being fuzzy numbers;

$\tilde{b} = (\tilde{b}_1, \tilde{b}_2, \ldots, \tilde{b}_m)$, $\tilde{b}_j > \tilde{0}, j = 1, 2, \ldots, m$; a vector with either all, some or no components being fuzzy numbers;

$\tilde{x} = (\tilde{x}_1, \tilde{x}_2, \ldots \tilde{x}_m)$, $\tilde{x}_i \geq \tilde{0}, i = 1, 2, \ldots, n$; a vector with either all, some or no components being fuzzy numbers;

$\tilde{A} = \left[\tilde{a}_{ij}\right]_{m \times n}$ matrix $m \times n, \tilde{a}_{ij} \in R, i = 1, 2, \ldots, n; j = 1, 2, \ldots, m$; all the elements of the matrix can be fuzzy numbers, or just some or none of the elements are fuzzy numbers.

Now let us change the fuzzy linear program (3.01) in such a way that in matrix $\tilde{A}$ part of the elements in some columns are unknown, but there is a demand that they are restricted with some given convex constraint. We split the matrix:

$$\tilde{A}=\begin{bmatrix}\tilde{a}_{11} & \tilde{a}_{12} & \cdots & \tilde{a}_{1n}\\ \tilde{a}_{21} & \tilde{a}_{22} & \cdots & \tilde{a}_{2n}\\ \vdots & \vdots & \cdots & \vdots\\ \tilde{a}_{m1} & \tilde{a}_{m2} & \cdots & \tilde{a}_{mn}\end{bmatrix}$$

in accordance with the columns into two parts:

$$\tilde{A}=\begin{bmatrix}\tilde{a}_{11} & \tilde{a}_{12} & \cdots & \tilde{a}_{1\mu} & \tilde{a}'_{1,\mu+1} & \tilde{a}'_{1,\mu+2}\cdots\tilde{a}'_{1n}\\ \tilde{a}_{21} & \tilde{a}_{22} & \cdots & \tilde{a}_{2\mu} & \tilde{a}'_{2,\mu+1} & \tilde{a}'_{2,\mu+2}\cdots\tilde{a}'_{2n}\\ \vdots & \vdots & \cdots & \vdots & \vdots & \vdots \quad \cdots \quad \vdots\\ \tilde{a}_{m1} & \tilde{a}_{m2} & \cdots & \tilde{a}_{m\mu} & \tilde{a}'_{m,\mu+1} & \tilde{a}'_{m,\mu'2}\cdots\tilde{a}'_{mn}\end{bmatrix}=\begin{bmatrix}\tilde{A}_0 \vdots \tilde{A}'\end{bmatrix}_{m\times n}$$

where:

$$\tilde{A}_0=\begin{bmatrix}\tilde{a}_{11} & \tilde{a}_{12} & \cdots & \tilde{a}_{1\mu}\\ \tilde{a}_{21} & \tilde{a}_{22} & \cdots & \tilde{a}_{2\mu}\\ \vdots & \vdots & \cdots & \vdots\\ \tilde{a}_{m1} & \tilde{a}_{m2} & \cdots & \tilde{a}_{m\mu}\end{bmatrix}=\begin{bmatrix}\tilde{P}_1 & \tilde{P}_2 & \cdots & \tilde{P}_\mu\end{bmatrix}$$

is a $m \times \mu$ matrix with the elements that are fuzzy numbers. Now denote with $\tilde{P}_j,\ j=1,2,\ldots,\mu$ the columns of matrix $\tilde{A}_0$.
In the matrix:

$$\tilde{A}'=\begin{bmatrix}\tilde{a}'_{1,\mu+1} & \tilde{a}'_{1,\mu+2}\cdots\tilde{a}'_{1n}\\ \tilde{a}'_{2,\mu+1} & \tilde{a}'_{2,\mu+2}\cdots\tilde{a}'_{2n}\\ \vdots & \vdots \quad \cdots \quad \vdots\\ \tilde{a}'_{m,\mu+1} & \tilde{a}'_{m,\mu'2}\cdots\tilde{a}'_{mn}\end{bmatrix}=\begin{bmatrix}\tilde{P}_{\mu+1} & \tilde{P}_{\mu+2} & \cdots & \tilde{P}_n\end{bmatrix}$$

the elements (in some columns) are currently unknown, but as well as coefficients in an objective function, they are bounded with some determined convex constraint.
Denote $\tilde{c}_j=\tilde{a}_{m+1}$, $j=1,2,\ldots,n$, and if we insert this into the row $(m+1)$ of matrix $\tilde{A}$ we obtain extended matrix $\hat{\tilde{A}}$:

$$\hat{\tilde{A}}=\begin{bmatrix}\tilde{a}_{11} & \tilde{a}_{12} & \cdots & \tilde{a}_{1\mu} & \tilde{a}'_{1,\mu+1} & \tilde{a}'_{1,\mu+2} & \cdots & \tilde{a}'_{1n}\\ \tilde{a}_{21} & \tilde{a}_{22} & \cdots & \tilde{a}_{2\mu} & \tilde{a}'_{2,\mu+1} & \tilde{a}'_{2,\mu+2} & \cdots & \tilde{a}'_{2n}\\ \vdots & \vdots & \cdots & \vdots & \vdots & \vdots & \cdots & \vdots\\ \tilde{a}_{m1} & \tilde{a}_{m2} & \cdots & \tilde{a}_{m\mu} & \tilde{a}'_{m,\mu+1} & \tilde{a}'_{m,\mu'2} & \cdots & \tilde{a}'_{mn}\\ \tilde{a}_{m+1,1} & \tilde{a}_{m+1,2} & \cdots & \tilde{a}_{m+1,\mu} & \tilde{a}'_{m+1,\mu+1} & \tilde{a}'_{m+1,\mu'2} & \cdots & \tilde{a}'_{m+1,n}\end{bmatrix}=\begin{bmatrix}\tilde{A}_0 \vdots \tilde{A}'\end{bmatrix}_{(m+1)\times n}$$

The columns:

$$\hat{\tilde{P}}_j = \begin{bmatrix} \tilde{a}'_{1j} \\ \tilde{a}'_{2j} \\ \vdots \\ \tilde{a}'_{mj} \\ \tilde{a}'_{m+1,j} \end{bmatrix}, j = \mu+1, \mu+2, \ldots, n;\ \tilde{a}'_{m+1,j} = \tilde{c}_j$$

are restricted with some determined convex composition $\hat{\tilde{P}}_j \in \tilde{C}_j$, $j = \mu+1, \mu+2, \ldots, n$, where $\tilde{C}_j$ is a fuzzy convex polyhedron, determined by given constraints. Thus, we obtain the generalised fuzzy linear program *[2]*:

$$\begin{aligned} & opt\left(\tilde{c}, \tilde{x}\right) \\ & \tilde{A}\tilde{x} = \tilde{b} \\ & \tilde{A} = \left[\tilde{A}_0 \vdots \tilde{A}'\right] \\ & \hat{\tilde{P}} \in \tilde{C}_j,\ j = \mu+1, \mu+2, \ldots, n \\ & \tilde{x} \geq \tilde{0} \end{aligned} \tag{3.02}$$

In the generalised fuzzy linear program (GFLP), we have to define the optimum of the objective function and simultaneously also compute the optimal structure of varying convexly linked columns $\hat{\tilde{P}}_j$, $j = \mu+1, \mu+2, \ldots, n$.

There are two phases in the procedure to solving the generalised linear programming problems *[1], [2], [5]*. The first phase means solving the program (3.02) without varying convexly linked columns, therefore in the first phase we set $\tilde{A}' \equiv O$ and thus obtain a standard fuzzy linear program, which can be solved using the simplex algorithm. In the second phase in each iteration, we add to the obtained optimal solution from the first phase additional conditions of varying convexly linked columns, and thus we obtain a generalisation of the original program using Wolfe's modified simplex method.

3.1 Main program

In program (3.02), we seek the optimal solution that can be either minimum or maximum. From the theory of linear programming, it is known that the procedure is the same in both cases.

In (3.02) we extend matrix $\tilde{A} = \left[\tilde{A}_0 \vdots \tilde{A}'\right]$ with row $(m+1)$ and denote this matrix with $\tilde{A} = \left[\hat{\tilde{A}}_0 \vdots \hat{\tilde{A}}'\right]$. Also, we introduce vectors P_0 and $\hat{\tilde{b}}$:

$$P_0 = \begin{bmatrix} 0 \\ 0 \\ \vdots \\ 0 \\ 1 \end{bmatrix}_{(m+1)\times 1} \qquad \hat{\tilde{b}} = \begin{bmatrix} \tilde{b} \\ 0 \end{bmatrix}_{(m+1)\times 1}$$

Now we denote $\tilde{z} = (\tilde{c}, \tilde{x}) = \tilde{z}_0$ and rewrite program (3.02) in this form:

$$\begin{aligned} &\max \tilde{x}_0 \\ &P_0 \tilde{x}_0 + \hat{\tilde{A}} \tilde{x} = \hat{\tilde{b}} \\ &\hat{\tilde{A}} = \left[\hat{\tilde{A}}_0 \ \vdots \ \hat{\tilde{A}}' \right]_{(m+1)\times n} \\ &\hat{\tilde{P}} \in \tilde{C}_j, \ j = \mu+1, \mu+2, \ldots, n \\ &\tilde{x} \geq \tilde{0} \end{aligned} \tag{3.03}$$

Definition: *Linear program of form (3.03) is called a* ***main program.***

Since we are using Dantzig simplex algorithm to solve this program, in each step, the row $(m+1)$ in inverse of the basis $P^{(k)}$ is a row of simplex multipliers:

$$\begin{aligned} \tilde{\pi}^{(k)} &= \left[-\tilde{\pi}_1 \ -\tilde{\pi}_2 \ \cdots \ -\tilde{\pi}_m \right] \\ \hat{\tilde{\pi}}^{(k)} &= \left[-\tilde{\pi}_1 \ -\tilde{\pi}_2 \ \cdots \ -\tilde{\pi}_m \ ; \ 1 \right] \end{aligned}$$

These simplex multipliers can be in general fuzzy numbers. Moreover, consider also:

$$\begin{aligned} &\hat{\tilde{\pi}}^{(k)} \cdot \hat{\tilde{P}}_j \equiv 0 \qquad j - \text{ basic index} \\ &\hat{\tilde{\pi}}^{(k)} \cdot \hat{\tilde{P}}_j \overset{>}{<} 0 \qquad j - \text{nonbasic index} \\ &\hat{\tilde{\pi}}^{(k)} \cdot P_0 = 1 \end{aligned} \tag{3.04}$$

3.2 Initial feasible solution

Solving of the generalised fuzzy linear program is based on Dantzig simplex algorithm and Wolfe's modified simplex method. Thus, we solve the problem in two phases. In the first phase we look for an optimal feasible basic solution to problem (3.03) without varying vectors $\hat{\tilde{P}}_j, \ j = \mu+1, \mu+2, \ldots, n$, i.e., a standard fuzzy linear program, which can be solved using the

Dantzig simplex algorithm. Solution $\tilde{x}^{(k_0)}$ is a vector with components that can be either fuzzy numbers or, in some cases, also regular real numbers. This depends on the type of fuzzy linear program that we are dealing with. The obtained solution $\tilde{x}^{(k_0)}$ is just a feasible basic solution for the main program (3.03) and in general not necessarily optimal. It is a starting point for computations in the second phase where we are seeking the solution of the main program (3.03). In the second phase we want to improve the solution obtained in the first phase. Into the basis we gradually bring vectors $\hat{\tilde{P}}_j$ considering convex constraints, i.e., $\hat{\tilde{P}}_j \in \tilde{C}_j$ for all $j = \mu+1, \mu+2, \ldots, n$.

3.3 First feasible solution

Let $\tilde{x}^{(k_0)}$ be the optimal solution of the first phase, which is for the second phase just the initial feasible basic solution, denoted by ${}^{(2)}\tilde{x}^{(0)}$. From the final simplex table of the first phase, we discern the row of simplex multipliers:

$$\hat{\tilde{\pi}}^{(0)} = \left[-\tilde{\pi}_1^{(0)} \ -\tilde{\pi}_2^{(0)} \ \cdots \ -\tilde{\pi}_m^{(0)} \ ; \ 1 \right]$$

After multiplying conditions of the main program (3.03) with these multipliers, we obtain

$$\hat{\tilde{\pi}}^{(0)} P_0 \tilde{x}_0 + \hat{\tilde{\pi}}^{(0)} \hat{\tilde{A}} x = \hat{\tilde{\pi}}^{(0)} \hat{\tilde{b}}$$

According to (3.04) we have:

$$\tilde{x}_0 + \sum_{j-nonbasic} \hat{\tilde{\pi}}^{(0)} \hat{\tilde{P}}_j x_j = \hat{\tilde{\pi}}^{(0)} \hat{\tilde{b}}$$

In the case where the optimum is a maximum and the value of function $\tilde{x}_0$ is optimal also for problem (3.03), there is $\hat{\tilde{\pi}}^{(0)} \hat{\tilde{P}}_j > 0$ for all non-basic indexes *j* and the problem is solved. If this is not the case, we have:

$$\hat{\tilde{\pi}}^{(k)} \hat{\tilde{P}}_j < 0, \ j \in I_1$$
$$I_1 - \textit{a set of nonbasic indexes}$$
$$I_1 \subseteq \{1, 2, \ldots, n\}$$

Since $\tilde{x}_0 = \hat{\tilde{\pi}}^{(0)} \hat{\tilde{b}} - \sum_{j-nonbasic} \hat{\tilde{\pi}}^{(0)} \hat{\tilde{P}}_j x_j$ the value of $\tilde{x}_0$ would be bigger if we find:

$$\min_j \hat{\tilde{\pi}}^{(0)} \hat{\tilde{P}}_j, \quad \hat{\tilde{P}}_j \in \tilde{C}_j \tag{3.05}$$

for all $j = \mu+1, \mu+2, \ldots, n$.

Problem (3.05) is called a ***system of first subprograms*** of the main program (3.03). For each unknown column we obtain one first subprogram, thus there will be as many first subprograms as there are unknown columns.

Allow the system of first subprograms to yield optimal solutions: $\hat{\tilde{\pi}}^{(0)}\hat{\tilde{P}}^{(1)}_{\mu+1}, \hat{\tilde{\pi}}^{(0)}\hat{\tilde{P}}^{(1)}_{\mu+2}, \ldots, \hat{\tilde{\pi}}^{(0)}\hat{\tilde{P}}^{(1)}_{n}$. In the case of real values, we choose the smallest (meaning we choose the value with the biggest absolute value). Assume that this is a solution with index λ_1 :

$$\min_j \hat{\tilde{\pi}}^{(0)}\hat{\tilde{P}}^{(1)}_{\mu+1} = \hat{\tilde{\pi}}^{(0)}\hat{\tilde{P}}^{(1)}_{\lambda_1},\ j = \mu+1, \mu+2, \ldots, n$$

In the case where these solutions are fuzzy numbers, we have to compare them using some ranking method. Dealing with triangular fuzzy numbers, it is appropriate to use the Chens method *[8]*.

As the most suitable to enter as the basis of the main program, of all the solutions: $\hat{\tilde{\pi}}^{(0)}\hat{\tilde{P}}^{(1)}_{\mu+1}, \hat{\tilde{\pi}}^{(0)}\hat{\tilde{P}}^{(1)}_{\mu+2}, \ldots, \hat{\tilde{\pi}}^{(0)}\hat{\tilde{P}}^{(1)}_{n}$ we choose the one that has in the process of ranking the biggest absolute value. Let this be the solution with index λ_1, i.e., $\min_j \hat{\tilde{\pi}}^{(0)}\hat{\tilde{P}}^{(1)}_{\mu+1} = \hat{\tilde{\pi}}^{(0)}\hat{\tilde{P}}^{(1)}_{\lambda_1},\ j = \mu+1, \mu+2, \ldots, n$.

In accordance with the Wolfe procedure, we return to the main program and write conditions with vectors $P_0, \hat{\tilde{P}}_1, \ldots, \hat{\tilde{P}}_n$ except $\hat{\tilde{P}}^{(1)}_{\lambda_1}$, which we substitute with the convex composition:

$$\hat{\tilde{P}}^{(1)}_{\lambda_1} = \left[\hat{\tilde{P}}^{(1)}_{\lambda_1} \cdot {}_{(1)}\tilde{x}_{\lambda_1} + \hat{\tilde{Q}}^{(\tilde{-}2)}_{\lambda_1} \cdot {}_{(2)}\tilde{x}_{\lambda_1} \right] \cdot \frac{1}{\tilde{x}_{\lambda_1}} \tag{3.06}$$

where we have:

$$\tilde{x}_{\lambda_1} = {}_{(1)}\tilde{x}_{\lambda_1} + {}_{(2)}\tilde{x}_{\lambda_1} \tag{3.07}$$

Formulation of convex composition (3.06) with condition (3.07) ensures that $\hat{\tilde{P}}^{(1)}_{\lambda_1} \in \tilde{C}_{\lambda_1}$. This means that we fixed $\hat{\tilde{P}}^{(1)}_{\lambda_1}$, thus we did not weaken the convex set $\tilde{C}_{\lambda_1}$, instead of $\hat{\tilde{P}}^{(1)}_{\lambda_1}$ we take $\hat{\tilde{Q}}^{(\tilde{-}2)}_{\lambda_1}$.

From the main program, the ***modified main program of the first degree*** is obtained:

$$\begin{aligned} &\max \tilde{x}_0 \\ &P_0\tilde{x}_0 + \sum_{j=1}^{n} \hat{\tilde{P}}_j\tilde{x}_j + \hat{\tilde{P}}^{(1)}_{\lambda_1} \cdot {}_{(1)}\tilde{x}_{\lambda_1} + \hat{\tilde{Q}}^{(2)}_{\lambda_1} \cdot {}_{(2)}\tilde{x}_{\lambda_1} = \hat{\tilde{b}} \\ &\hat{\tilde{P}} \in \tilde{C}_j,\ j = \mu+1, \mu+2, \ldots, n;\ j \neq \lambda_1 \end{aligned} \tag{3.08}$$

$$\hat{\tilde{P}}_{\lambda_1}^{(1)}, \hat{\tilde{Q}}_{\lambda_1}^{(-2)} \in \tilde{C}_{\lambda_1}$$
$$\tilde{x}_j \geq \tilde{0},\ j \neq 0,\ {}_{(1)}\tilde{x}_{\lambda_1} \geq \tilde{0},\ {}_{(2)}\tilde{x}_{\lambda_1} \geq \tilde{0}$$

Expression (3.06) can be written also in the form:

$$\hat{\tilde{P}}_{\lambda_1}^{(1)} \cdot \tilde{x}_{\lambda_1} = \hat{\tilde{P}}_{\lambda_1}^{(1)} \cdot {}_{(1)}\tilde{x}_{\lambda_1} + \hat{\tilde{Q}}_{\lambda_1}^{(-2)} \cdot {}_{(2)}\tilde{x}_{\lambda_1} \qquad (3.09)$$
$$\tilde{x}_{\lambda_1} = {}_{(1)}\tilde{x}_{\lambda_1} + {}_{(2)}\tilde{x}_{\lambda_1}$$

In (3.09), a $\hat{\tilde{P}}_{\lambda_1}^{(1)}$ is a new vector that enters the basis, thus the conditions in program (3.08) in accordance with the main program (3.03) are not demolished. Therefore, programs (3.08) and (3.03) are equivalent. Vector $\hat{\tilde{P}}_{s_1^{(1)}}^{(1)}$ that leaves the basis is determined using the usual procedure of the simplex algorithm, i.e. criterion of minimal quotient of positive elements of entering column $\hat{\tilde{P}}_{\lambda_1}^{(1)}$ with equilateral coefficients of the right-hand sides. In the case when elements of the entering column $\hat{\tilde{P}}_{\lambda_1}^{(1)}$ and/or right-hand side coefficients $\hat{\tilde{b}}_i, i = 1,2,\ldots,m$ are fuzzy numbers, it is necessary for both columns to first compute its ranking functions and then compute the corresponding quotients.
After the first iteration is done, all the $\tilde{c}_j$ are non-negative in the basic problem (3.03). By this action we obtain the first basic feasible solution of the main program, written as ${}^{(2)}\tilde{x}^{(1)} = \left[L_1^{(1)}\right]^{-1} \cdot \hat{\tilde{b}}^{(0)}$.

3.4 Further feasible solutions

From the basis $\hat{L}_1^{(1)}$ and its corresponding inverse $\left[\hat{L}_1^{(1)}\right]^{-1}$ we obtain new simplex multipliers in the last row, i.e., $\hat{\tilde{\pi}}^{(1)} = \left[-\tilde{\pi}_1^{(1)}\ -\tilde{\pi}_2^{(1)}\ \cdots\ -\tilde{\pi}_m^{(1)}\ ;\ 1\right]$. Here we have:

$$\hat{\tilde{\pi}}^{(1)} \cdot \hat{\tilde{P}}_j \geq \tilde{0},\ \ j = 1,2,\ldots,\mu$$
$$\hat{\tilde{\pi}}^{(1)} \cdot \hat{\tilde{P}}_{s_1^{(1)}}^{(1)} = 0$$

where $\hat{\tilde{P}}_{s_1^{(1)}}^{(1)}$ is a new basic vector.

Afterwards, we repeat the same iteration as previously and get the problem that we call ***system of second subprograms***:

$$\min_i \hat{\tilde{\pi}}^{(1)} \cdot \hat{\tilde{P}}_j \qquad \min_i \hat{\tilde{\pi}}^{(1)} \cdot \hat{\tilde{Q}}^{(2)}_{s_1}$$
$$\hat{\tilde{P}}_j \in \tilde{C}_j \qquad \hat{\tilde{Q}}^{(2)}_{s_1} \in \tilde{C}_{s_1}$$
$$j = \mu+1, \mu+2, \ldots, n; j \neq s_1^{(1)}$$
$$i = 1, 2, \ldots m$$

The process is similar to seeking the first solution. Namely, we find all solutions of the system of the second subprograms, then choose the minimum average from them, and then initiate the corresponding column into the basis of the main program. This yields a modified main program of the second degree, a subsequently modified program of the third degree, and so forth.

In general, in the *k*-th step we obtain a ***modified main program of degree (k-1)***:

$$\begin{aligned}
&\max \tilde{x}_0 \\
&P_0\tilde{x}_0 + \sum_{j=1}^{\mu} \hat{\tilde{P}}_j \tilde{x}_j + \sum_{s_j} \left(\sum_{\varepsilon=1}^{k-1} \hat{\tilde{P}}^{(\varepsilon)}_{s_j} \cdot {}_{(\varepsilon)}\tilde{x}_{s_j} + \sum_{\varepsilon=1}^{k-1} \hat{\tilde{Q}}^{(\varepsilon+1)}_{s_j} \cdot {}_{(\varepsilon+1)}\tilde{x}_{s_j} \right) = \hat{\tilde{b}} \\
&s_j \in I_2 \subseteq \{\mu+1, \mu+2, \ldots, n\} \\
&\hat{\tilde{P}} \in \tilde{C}_j,\ j \in \{\mu+1, \mu+2, \ldots, n\} - I_2 \\
&\hat{\tilde{P}}^{(\varepsilon)}_{s_j}, \hat{\tilde{Q}}^{(\varepsilon+1)}_{s_j} \in \tilde{C}_{s_j},\ s_j \in I_2 \\
&\tilde{x}_j \geq \tilde{0},\ j \neq 0,\ {}_{(\varepsilon)}\tilde{x}_{s_j} \geq \tilde{0},\ {}_{(\varepsilon+1)}\tilde{x}_{s_j} \geq \tilde{0}
\end{aligned} \tag{3,10}$$

Assume that while solving the program (3.10) we find a basic feasible solution ${}^{(2)}\tilde{x}^{(k-1)}$. This solution corresponds to basis $\hat{L}^{(k-1)}$ and its corresponding inverse $\left[\hat{L}^{(k-1)}\right]^{-1}$. The last row in this inverse is the row of simplex multipliers: $\hat{\tilde{\pi}}^{(k-1)} = \left[-\tilde{\pi}_1^{(k-1)} \ -\tilde{\pi}_2^{(k-1)} \ \cdots \ -\tilde{\pi}_m^{(k-1)} \ ; \ 1\right]$

According to definition of the simplex algorithm we have:

$$\hat{\tilde{\pi}}^{(k-1)} \cdot \hat{\tilde{P}}_j \geq 0 \qquad j = 1, 2, \ldots, \mu$$
$$\hat{\tilde{\pi}}^{(k-1)} \cdot \hat{\tilde{P}}_j^{(k-1)} = 0 \quad j \in \{1, 2, \ldots, n\} \quad , j - \text{basic index}$$
$$\hat{\tilde{\pi}}^{(k-1)} \cdot P_0 = 1$$
$$\hat{\tilde{\pi}}^{(k-1)} \cdot \hat{\tilde{P}}_j^{(k-1)} < 0 \quad j \in \{\mu+1, \mu+2, \ldots, n\} \quad , j - \text{nonbasic index}$$

From the $(k-1)$-th solution we attain the *k*-th solution, if we manage to solve the ***system of k-th subprograms***:

$$\min_i \hat{\tilde{\pi}}^{(k-1)} \cdot \hat{\tilde{P}}_j^{(k-1)} \qquad \min_i \hat{\tilde{\pi}}^{(k-1)} \cdot \hat{\tilde{Q}}_{s_j}^{(k)}$$
$$\hat{\tilde{P}}_j^{(k-1)} \in \tilde{C}_j \qquad \hat{\tilde{Q}}_{s_j}^{(k)} \in \tilde{C}_{s_j}$$
$$j \in \{1,2,\ldots,n\} - I_2 \qquad s_j \in I_2$$
$$I_2 \subseteq \{\mu+1, \mu+2, \ldots, n\}$$

From here we obtain the ***modified main program of degree k***:

$$\max \tilde{x}_0$$
$$P_0\tilde{x}_0 + \sum_{j=1}^{\mu} \hat{\tilde{P}}_j \tilde{x}_j + \sum_{s_j} \left(\sum_{\varepsilon=1}^{k-1} \hat{\tilde{P}}_{s_j}^{(\varepsilon)} \cdot {}_{(\varepsilon)}\tilde{x}_{s_j} + \sum_{\varepsilon=1}^{k-1} \hat{\tilde{Q}}_{s_j}^{(\varepsilon+1)} \cdot {}_{(\varepsilon+1)}\tilde{x}_{s_j} \right) + \hat{\tilde{P}}_{s_k}^{(k)} \cdot {}_{(k)}\tilde{x}_{s_k} + \hat{\tilde{Q}}_{s_k}^{(k+1)} \cdot {}_{(k+1)}\tilde{x}_{s_k} = \hat{\tilde{b}}$$
$$s_k, s_j \in I_2 \subseteq \{\mu+1, \mu+2, \ldots, n\}$$
$$\hat{\tilde{P}}_j \in \tilde{C}_j,\ j \in \{\mu+1, \mu+2, \ldots, n\} - I_2$$
$$\hat{\tilde{P}}_{s_j}^{(\varepsilon)}, \hat{\tilde{Q}}_{s_j}^{(\varepsilon+1)} \in \tilde{C}_{s_j},\ s_j \in I_2$$
$$\tilde{x}_j \geq \tilde{0},\ j \neq 0,\ {}_{(\varepsilon)}\tilde{x}_{s_j} \geq \tilde{0},\ {}_{(k)}\tilde{x}_{s_k} \geq \tilde{0},\ {}_{(k)}\tilde{x}_{s_k} \geq \tilde{0},\ {}_{(k+1)}\tilde{x}_{s_k} \geq \tilde{0} \tag{3.11}$$

3.5 The existence of the optimal solution

We proceed with the described steps as long as we can improve the value of objective function $\tilde{x}_0$. We obtain the optimal feasible solution on the k_0 -th step only when in the modified main program of degree k_0, and the vector of simplex multipliers $\hat{\tilde{\pi}}_i^{(k_0)}, i = 1,2,\ldots,p_{k_0}$ fulfil:

$$\hat{\tilde{\pi}}^{(k_0)} \cdot \hat{\tilde{P}}_j \geq 0 \qquad ,j = 1,2,\ldots,\mu$$
$$\hat{\tilde{\pi}}^{(k_0)} \cdot \hat{\tilde{P}}_j^{(k_0)} = 0 \quad ,j \in \{\mu+1, \mu+2, \ldots, n\} \quad ,j - \text{basic index}$$
$$\hat{\tilde{\pi}}^{(k_0)} \cdot P_0 = 1$$
$$\hat{\tilde{\pi}}^{(k_0)} \cdot \hat{\tilde{P}}_j^{(k_0)} \geq 0 \quad ,j \in \{\mu+1, \mu+2, \ldots, n\} \quad ,j - \text{nonbasic index}$$

In this circumstance, in the system of (k_0+1) - th subprograms:

$$\min_i \hat{\tilde{\pi}}^{(k_0)} \cdot \hat{\tilde{P}}_j^{(k_0)}$$
$$\hat{\tilde{P}}_j^{(k_0)} \in \tilde{C}_j$$
$$j \in \{\mu+1, \mu+2, \ldots, n\}$$

we cannot find any product $\hat{\tilde{\pi}}^{(k_0)} \cdot \hat{\tilde{P}}_j^{(k_0)}$ that is negative, and therefore it is impossible to bring such a vector into the basis of the main program that would improve the value of objective function $\tilde{x}_0$. Thus, we have found the optimal solution of program (3.02), since program (3.02) and modified main program (3.11) are equivalent and therefore have the same optimal solution.

3.6 Degenerate solution

In the given algorithm, degeneracy is also possible. The approach for solving problems in such cases is briefly described in *[2].*

4 NUMERICAL EXAMPLE

We want to solve the problem:

$$\begin{aligned}
\min z = {} & 2x_1 + 6x_2 + 8x_3 + 5x_4 + c_5 x_5 + c_6 x_6 \\
& 4x_1 + x_2 + 2x_3 + 2x_4 + a'_{15}x_5 + a'_{16}x_6 \geq (78, 80, 82) \\
& 2x_1 + 5x_2 \qquad + 4x_4 + a'_{25}x_5 + a'_{26}x_6 \geq 40 \\
& \qquad 2x_2 + 4x_3 + x_4 + a'_{35}x_5 + a'_{36}x_6 \geq (118, 120, 122) \\
& x_i \geq 0, i = 1,2,3,4,5,6
\end{aligned}$$

with the given convex restriction of varying columns $\hat{P} \in C_5$, $\hat{P}_6 \in C_6$.

$$C_5 : \begin{cases} a'_{15} + a'_{25} + a'_{35} - a'_{45} = 3 \\ 2a'_{15} + 5a'_{25} + a'_{35} + 3a'_{45} = (9, 10, 11) \\ a'_{i5} \geq 0, \ i = 1,2,3,4 \end{cases}$$

$$C_6 : \begin{cases} 2a'_{16} + a'_{26} + a'_{36} + 2a'_{46} = (5, 6, 7) \\ 4a'_{16} + 2a'_{26} + 2a'_{36} - 4a'_{46} = 8 \\ a'_{i6} \geq 0, \ i = 1,2,3,4 \end{cases}$$

We solve this problem in two phases: in the first phase we solve the linear program without varying columns, and in the second phase we deal with systems of subprograms.

Main program

$$\max x_0$$

$$P_0 x_0 + \hat{P}_1 x_1 + \hat{P}_2 x_2 + \hat{P}_3 x_3 + \hat{P}_4 x_4 + \hat{P}_5 x_5 + \hat{P}_6 x_6 = \hat{\hat{b}}$$

$$P_0 = \begin{bmatrix} 0 \\ 0 \\ 0 \\ 1 \end{bmatrix}, \hat{P}_1 = \begin{bmatrix} 4 \\ 2 \\ 0 \\ 2 \end{bmatrix}, \hat{P}_2 = \begin{bmatrix} 1 \\ 5 \\ 2 \\ 6 \end{bmatrix}, \hat{P}_3 = \begin{bmatrix} 2 \\ 0 \\ 4 \\ 8 \end{bmatrix}, \hat{P}_4 = \begin{bmatrix} 2 \\ 4 \\ 1 \\ 5 \end{bmatrix}, \hat{P}_5 = \begin{bmatrix} a'_{15} \\ a'_{25} \\ a'_{13} \\ a'_{45} \end{bmatrix}, \hat{P}_6 = \begin{bmatrix} a'_{16} \\ a'_{26} \\ a'_{16} \\ a'_{46} \end{bmatrix}$$

Initial main program without varying columns is of the form:

$$\begin{aligned} \min z = {} & 2x_1 + 6x_2 + 8x_3 + 5x_4 \\ & 4x_1 + x_2 + 2x_3 + 2x_4 \geq (78, 80, 82) \\ & 2x_1 + 5x_2 \quad\quad + 4x_4 \geq 40 \\ & \quad\quad 2x_2 + 4x_3 + x_4 \geq (118, 120, 122) \\ & x_i \geq 0, i = 1, 2, 3, 4, 5, 6 \end{aligned}$$

The fuzzy solution of the initial main program is *[2]:*

$$\tilde{x}_1 = (4.75, 5, 5.25) \quad \tilde{x}_2 = (6.1, 6, 5.9) \quad \tilde{x}_3 = (26.45, 27, 27.55) \quad \tilde{x}_4 = (0, 0, 0)$$

$$\tilde{z}_{\min} = (257.7, 262, 266.3) \quad \hat{\pi}^{(0)} = [-0.3, \ -0.4, \ -1.85 \ \vdots \ 1]$$

We obtain the system of the first subprograms:

a) For vector $\hat{\hat{P}}_5$:

$$\begin{aligned} \min \hat{\pi}^{(0)} \hat{\hat{P}}_5 = {} & -0,3a'_{15} - 0,4a'_{25} - 1,85a'_{35} + a'_{45} \\ & a'_{15} + \quad a'_{25} + \quad a'_{35} - a'_{45} = 3 \\ & 2a'_{15} + \quad 5a'_{25} + \quad a'_{35} + \quad 3a'_{45} = (9, 10, 11) \end{aligned}$$

Solution:

$$\hat{\hat{P}}_5 = \begin{bmatrix} 0 \\ 0 \\ (4.5, 4.75, 5) \\ (1.5, 1.75, 2) \end{bmatrix}, \quad \min \hat{\pi}^{(0)} \hat{\hat{P}}_5 = (-6.825, -7.0375, -7.25)$$

b) For vector $\hat{\hat{P}}_6$

$$\begin{aligned} \min \hat{\pi}^{(0)} \hat{\hat{P}}_6 = {} & -0,3a'_{16} - 0,4a'_{26} - 1,85a'_{36} + a'_{46} \\ & 2\,a'_{16} + \quad a'_{26} + \quad a'_{36} + 2\,a'_{46} = (5, 6, 7) \\ & 4a'_{16} + \quad 2a'_{26} + \quad 2a'_{36} - 4a'_{46} = 8 \end{aligned}$$

Solution:

$$\hat{\tilde{P}}_5 = \begin{bmatrix} 0 \\ 0 \\ (4.5, 4.75, 5) \\ (1.5, 1.75, 2) \end{bmatrix}, \quad \min \hat{\pi}^{(0)} \hat{\tilde{P}}_5 = (-6.825, -7.0375, -7.25)$$

b) For vector $\hat{\tilde{P}}_6$

$$\min \hat{\pi}^{(0)} \hat{\tilde{P}}_6 = -0,3a'_{16} - 0,4a'_{26} - 1,85a'_{36} + a'_{46}$$
$$2\,a'_{16} + a'_{26} + a'_{36} + 2\,a'_{46} = (5, 6, 7)$$
$$4a'_{16} + 2a'_{26} + 2a'_{36} - 4a'_{46} = 8$$

Solution:

$$\hat{\tilde{P}}_6 = \begin{bmatrix} 0 \\ 0 \\ (4.5, 5, 5.5) \\ (0.25, 0.5, 0.75) \end{bmatrix}, \quad \min \hat{\pi}^{(0)} \hat{\tilde{P}}_6 = (-8.075, -8.75, -9.425)$$

We rank both solutions, and after considering $R\left(\hat{\pi}^{(0)} \hat{\tilde{P}}_6\right) > R\left(\hat{\pi}^{(0)} \hat{\tilde{P}}_5\right)$, we choose column $\hat{\tilde{P}}_6$ to move to the basis of the main program of the first degree.

Modified main program of the first degree:

$$\max x_0$$

$$P_0\tilde{x}_0 + \hat{P}_1\tilde{x}_1 + \hat{P}_2\tilde{x}_2 + \hat{P}_3\tilde{x}_3 + \hat{P}_4\tilde{x}_4 + \hat{P}_5\tilde{x}_5 + \left(\hat{\tilde{P}}_6^{(1)} \cdot {}_{(1)}\tilde{x}_6 + \hat{\tilde{Q}}_6^{(2)} \cdot {}_{(2)}\tilde{x}_6\right) = \hat{\tilde{b}}$$

$$P_0 = \begin{bmatrix} 0 \\ 0 \\ 0 \\ 1 \end{bmatrix}, \hat{P}_1 = \begin{bmatrix} 4 \\ 2 \\ 0 \\ 2 \end{bmatrix}, \hat{P}_2 = \begin{bmatrix} 1 \\ 5 \\ 2 \\ 6 \end{bmatrix}, \hat{P}_3 = \begin{bmatrix} 2 \\ 0 \\ 4 \\ 8 \end{bmatrix}, \hat{P}_4 = \begin{bmatrix} 2 \\ 4 \\ 1 \\ 5 \end{bmatrix}, \hat{P}_5 = \begin{bmatrix} a'_{15} \\ a'_{25} \\ a'_{13} \\ a'_{45} \end{bmatrix},$$

$$\hat{\tilde{P}}_6^{(1)} = \begin{bmatrix} 0 \\ 0 \\ (4.5, 5, 5.5) \\ (0.25, 0.5, 0.75) \end{bmatrix}, \hat{\tilde{Q}}_6^{(2)} = \begin{bmatrix} a'_{16} \\ a'_{26} \\ a'_{16} \\ a'_{46} \end{bmatrix}$$

has the solution:

$$\tilde{z}_{\min} = (51.8, 52, 53.2)$$
$$\tilde{x}_1 = (20, 20, 20.5)$$
$$x_2 = x_3 = x_4 = 0$$
$${}_{(1)}\tilde{x}_6 = (23.6, 24, 24.4)$$
$$\hat{\tilde{\pi}}^{(1)} = \left[(0, -0.5, -0, 5), (-1, 0, 0,), (-0.1, -0.1. - 0, 1); 1\right]$$

We continue with the steps and attain an **optimal solution,** which is a result of the modified main program of degree 6.

$$z_{\min} = (31.4, 32.0, 32.6)$$
$$x_1 = x_2 = x_3 = x_4 = 0$$
$${}_{(3)}x_5 = {}_{(1)}x_6 = {}_{(2)}x_6 = 0$$
$${}_{(4)}\tilde{x}_6 = (8,8,8)$$
$${}_{(5)}\tilde{x}_6 = (31.2,32.0,32.8)$$
$${}_{(6)}\tilde{x}_6 = (23.6,24.0,24.4)$$

Decision variable $x_5 = {}_{(3)}x_5 = 0$, decision variable x_6 in the optimal solution is composed as:

$$\tilde{x}_6 = {}_{(4)}\tilde{x}_6 + {}_{(5)}\tilde{x}_6 + {}_{(6)}\tilde{x}_6 = (8,8,8) + (31.2,32,32.8) + (23.6,24.0,24.4) = (62.8,64.0,65.2)$$

The columns $\hat{\hat{P}}_5$ and $\hat{\hat{P}}_6$ are:

$$\hat{\hat{P}}_5 = \hat{\hat{P}}_5^{(3)} = \begin{bmatrix} (3.6,3.8,4) \\ 0 \\ 0 \\ (0.6,\ 0.8,\ 1) \end{bmatrix} \quad \hat{\hat{P}}_6 = \begin{bmatrix} (1.118,1.25,1.383) \\ (0.573,0.625,0.675) \\ (1.691,1.875,2.058) \\ (0.25,0.50,0.75) \end{bmatrix}$$

The original fuzzy linear program that also includes columns $\hat{\hat{P}}_5$ and $\hat{\hat{P}}_6$ is now:

$$\begin{aligned} \min z = {} & 2x_1 + 6x_2 + 8x_3 + 5x_4 + (0.6,\ 0.8,\ 1)\cdot x_5 + (0.25,0.50,0.75)\cdot x_6 \\ & 4x_1 + x_2 + 2x_3 + 2x_4 + (3.6,3.8,4)\cdot x_5 + (1.118,1.25,1.383)\cdot x_6 \geq (78,80,82) \\ & 2x_1 + 5x_2 \quad + 4x_4 + \quad (0.573,0.625,0.675)\cdot x_6 \geq 40 \\ & \quad 2x_2 + 4x_3 + x_4 + \quad (1.691,1.875,2.058)\cdot x_6 \geq (118,120,122) \\ & x_i \geq 0,\ i = 1,2,3,4,5,6 \end{aligned}$$

5 CONCLUSIONS

Generalisation of a linear program using Wolfe's modified simplex method is also possible and reasonable for fuzzy linear programming. Computational stages are based on a theoretical algorithm that demands multiple iterations of a two-phase procedure. In the first phase we find a solution for the modified main program, and in the second phase we solve the system of subprograms, where we determine the entering vector for basis. The use of simplex multipliers requires the well-known Dantzig simplex algorithm, which can be easily solved using several computer software programs. Dealing with a linear program where some or even all coefficients are fuzzy numbers still represents a challenge. In this case we must apply one of the methods found in *[2].*

The following research opens up a wide range of possibilities by introducing dynamics, i.e., taking into account the time component in fuzzy numbers/sets. Fuzzy sets describing a fuzzy linear program in this case become dependent on time: $\tilde{A}(t), \tilde{c}(t), \tilde{b}(t)$ and $\tilde{x}(t),\ t \in [0,T], T < +\infty$.

An extended application of fuzzy linear programming and its generalisation in actual real-life problems depend on powerful computer software capable of solving such problems. Unfortunately, such software does not yet exist.

References

[1] **G.B. Dantzig:** *Linear Programming and Extensions,* Princeton University Press, Princeton, New Jersey, 1998), eleventh printing.

[2] **J. Usenik and M. Žulj:** *Generalizirano mehko linearno programiranje,* Novo mesto: Fakulteta za organizacijske študije, 2021.

[3] **V. Rupnik:** *Zvezno dinamično linearno programiranje*, Ekonomska, poslovna in organizacijska knjižnica, 24, Založba Obzorja Maribor, Maribor, 1978.

[4] **J. Usenik**: Fuzzy dynamic linear programming in energy supply planning, *Journal of energy technology*, Oct. 2011, vol. 4, iss. 4, pp. 45–62.

[5] **J. Usenik:** *Generalizirano zvezno variabilno dinamično linearno programiranje,* Novo mesto: Fakulteta za industrijski inženiring, 2017.

[6] **L. A. Zadeh:** *Fuzzy sets*, Information and control, 8(3):338–353, 1965

[7] **H.-J. Zimmermann:** *Fuzzy Set Theory and its Applications*, Kluwer Academic Publishers (2001), Fourth edition.

[8] **S. Chen, C. Hwang, P. Hwang**: *Fuzzy Multiple Attribute Decision Making,* Springer-Verlag, (Berlin, Heidelberg, New York, 1992).

[9] **M. Repnik and D. Bokal***: A Basis for Taxonomy of Fuzzy Linear Programming Methods,* In 13th International Symposium on Operational Research in Slovenia, Bled, Slovenia, September 23-25, 2015. ZADNIK STIRN, Lidija (ur.), et al. SOR '15 proceedings, pages 188–192. Ljubljana: Slovenian Society Informatika, Section for Operational Research, 2015

Journal of Energy Technology

JET Volume 16 (2023) p.p. 41-50
Issue 1, 2023
Type of article: 1.01
http://www.fe.um.si/si/jet.htm

ASSESSMENT OF HUMAN EXPOSURE TO ELECTRIC AND MAGNETIC FIELDS NEAR TRANSMISSION LINES USING FEMM

OCENA IZPOSTAVLJENOSTI ČLOVEKA ELEKTRIČNIM IN MAGNETNIM POLJEM V BLIŽINI DALJNOVODOV Z UPORABO FEMM

Bojan Glushica[1ℜ], Blagoja Markovski[1], Andrijana Kuhar[1], Vesna Arnautovski Toseva[1]

Keywords: finite elements method, transmission lines, electric field, magnetic field, electromagnetic computation

Abstract

The intensity of ELF electric and magnetic fields near transmission lines is of particular interest in environmental and equipment protection studies. The use of numerical tools is the most efficient method for their assessment. In this paper, we numerically compute the electric and magnetic fields near different configurations of high-voltage transmission lines using the open- source software FEMM 4.2. Computed fields are compared with reference levels related to human exposure to electromagnetic fields. The accuracy of the applied method is validated with published, numerically computed and measured results.

ℜ Corresponding author: M.Sc. Bojan Glushica, Ss. Cyril and Methodius University in Skopje, Faculty of Electrical Engineering and Information Technologies, Rugjer Boshkovikj 18, Skopje 1000, North Macedonia, Tel.: +389 71 326 521, E-mail address: glushica@feit.ukim.edu.mk

1 Ss. Cyril and Methodius University in Skopje, Faculty of Electrical Engineering and Information Technologies, Rugjer Boshkovikj 18, Skopje 1000, North Macedonia

Povzetek

Intenzivnost električnih in magnetnih polj ELF v bližini daljnovodov je še posebej zanimiva za študije, ki so povezane z zaščito okolja in opreme. Uporabo numeričnih orodij lahko štejemo kot najučinkovitejšo metodo za njihovo ocenjevanje. V članku podamo prikaz numerično izračunanega električnega in magnetnega polja v bližini različnih konfiguracij visokonapetostnih daljnovodov z uporabo odprtokodne programske opreme FEMM 4.2. Izračunana elektromagnetna polja nato primerjamo z referenčnimi ravnmi, ki so povezane z izpostavljenostjo človeka elektromagnetnim poljem. Na koncu potrdimo natančnost uporabljene metode s podanimi numerično izračunanimi in merilnimi rezultati.

1 INTRODUCTION

Overhead transmission lines (OTL) generate extremely low frequency (ELF) electric and magnetic fields that may interact with technical or biological systems and produce possible harmful effects in case of excessive exposure [1], [2]. Therefore, the intensity and distribution of electric and magnetic fields near OTL are of particular interest in studies related to their possible adverse effects on the environment, human health, sensitive electronic equipment and critical infrastructures. To address the variety of problems that can occur, numerous standards and protocols have been introduced that define methods for assessment and protection from the effects of electromagnetic fields [3]-[5]. The use of electromagnetic simulation tools can be considered the most efficient method, especially when dealing with large and complex systems where measuring procedures can be time-consuming, expensive or impractical. Another advantage of the simulation tools is in the possibility of analysing systems in the initial phase of their planning and construction, and the ability to test the effectiveness of different protection techniques.

In this paper, we perform numerical analysis of the intensity and distribution of ELF electric and magnetic fields in the vicinity of OTL using the open-source software for analysing electromagnetic problems, FEMM 4.2, which is based on the finite element method (FEM) [6]-[8]. The modelling procedure is briefly described and validated using a full-wave electromagnetic model based on the method of moments (MoM) and by comparison of published and measured results. The analysis should provide general information for the expected field levels near 110 kV and 400 kV OTL. Therefore, different configurations of OTL and effectiveness of phase sequence transposition in double-circuit OTL are considered. Computed electric and magnetic field levels are compared with reference levels for human exposure to electromagnetic fields, established by the International Commission on Non-Ionizing Radiation Protection (ICNIRP) [9].

2 PROCEDURES FOR MODELLING THE ELECTROMAGNETIC PROBLEM IN FEMM

Modelling electromagnetic problems in open space using the FEMM 4.2 software requires specifying a solution domain with suitable shape and size for the analysed problem and appropriate boundary conditions at its borders. The solution domain, in which the electromagnetic problem is solved, should have a circular shape. Since the height of the analysed OTL is nearly 40 m, to reduce the boundary's influence, the domain's radius is set to 300 m, which is more than seven

times larger than the height of the analysed OTL. The domain is divided into two sections. The bottom section is ground, with specific conductivity σ, and the top section is air. The horizontal position of the OTL is at the centre of the domain (corresponding to distance of 0 m in the figures). Because the field computation is a time-consuming process and because we focus on the fields above the ground in the vicinity of the conductors, the discretization of the solution domain is done separately in sections, as shown in Fig. 1. The ground has the lowest degree of discretization. The air is divided into two half circles with 150 m and 300 m radius, where the inner circle has the highest degree of discretization to obtain more accurate results. The solution domain is discretized with about 340,000 nodes or 685,000 elements.

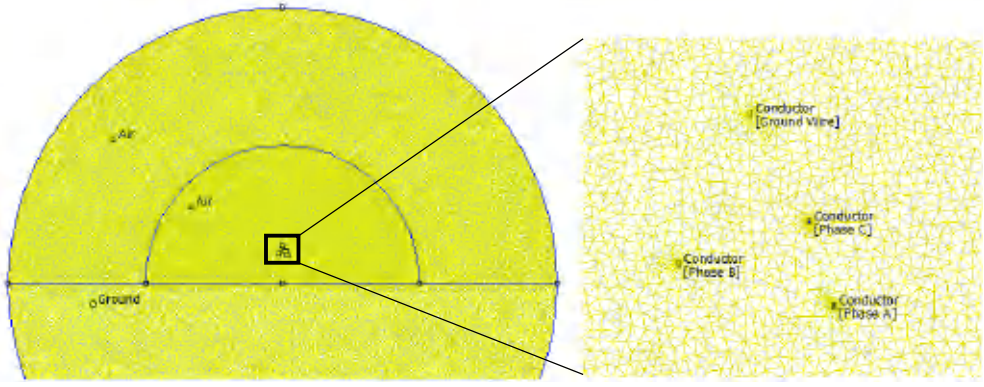

Figure 1: *Different degrees of discretization for the 110 kV single-circuit transmission line*

The FEMM 4.2 software provides instantaneous values of computed fields (electric or magnetic), while RMS values are further required to estimate human exposure to electromagnetic fields *[9]*. To obtain the RMS values, we compute multiple samples of the instantaneous field values over one period of 20 ms. We have observed that 40 equally spaced samples over one period can provide a good estimate of the RMS values of the 50 Hz fields. To automate this process for all considered cases, we have used the Lua scripting language which is incorporated in the FEMM 4.2 software. The electric and magnetic fields are computed at multiple points at a height of 1 m above ground level, along a profile perpendicular to the centre of the transmission line, as required by the standard [3]. The above-mentioned procedures are general for calculating electric and magnetic fields. In the following subsections, we describe some specific procedures for computing the electric magnetic fields.

2.1 Procedures for obtaining the RMS electric field

The electric field and scalar potential are computed using the “Current Flow” module of FEMM 4.2. For this module, fixed voltages are required. The boundary condition for potentials at the domain’s borders is set to 0 V. The same condition is applied for the ground wires. The phase conductors are set to instantaneous phase voltages that correspond to the appropriate time points within one period of 20 ms using a Lua script. Two cases are observed for the double-circuit power line: in the first case the phase conductors are untransposed, and in the second case they are transposed. The relative dielectric permittivity of the whole domain is $\varepsilon_1 = 1$.

2.2 Procedures for obtaining the RMS magnetic field

The magnetic field and magnetic vector potential are computed using FEMM 4.2's "Magnetics" module. A fixed current strength and magnetic vector potential are required for this module. The boundary condition for the magnetic vector potential at the domain's borders is set to 0 Wb/m. The current strength in the ground wire is forced at 0 A. The maximum load current of the TL is considered for the current strength in the phase conductors. The instantaneous values for the current strength of each phase are set based on the time points using a Lua script. For the double-circuit power line, the untransposed and transposed cases are considered as well. The relative magnetic permeability of the whole domain is $\mu_r = 1$.

3 VALIDATION OF THE APPLIED METHOD

In this section, we validate the accuracy of the applied method by comparison with published and numerically computed results.

3.1 Validation with published results

Validation of the procedures presented in Section 2 is performed by comparing the simulated results and the results provided in the European standard IEC 62110:2009 [3] for the geometries and conditions provided in the standard. For the OTL, a 77 kV transposed double-circuit is considered. The current strength is assumed to be 200 A. The same geometry provided in Table 2 and Fig. 6 for the transposed double-circuit OTL without the ground wire is used (as specified in the standard [3]). The ground clearance is h_g = 11 m. The results are shown in Fig. 2. The differences in the simulated and provided electric and magnetic field levels at 1 m above ground level are observed to be less than 5%.

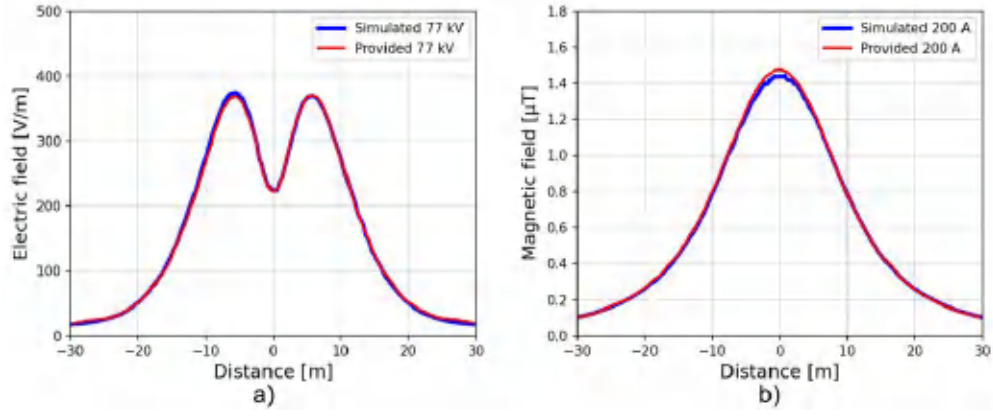

Figure 2: *Comparison between simulated and published results (in [3], Fig. A.5 and Fig. B.3) for a) RMS electric field and b) RMS magnetic field for double-circuit OTL*

The simulated magnetic field is also validated for underground transmission lines (UTL). A similar approach, as described in Section 2.2, is used with different discretization levels around

the phase conductors. Double-circuit configuration with balanced 200 A current strength is considered. The phase conductors are placed vertically on the same axis with 0.35 m separation, while the horizontal separation between the two circuits is 1 m (as specified in the standard [3]). The magnetic field levels at 1 m above ground level were calculated for two different distances between the UTL and ground level: h_g = 1.85 m and h_g = 0.6 m. The results of this simulation are shown in Fig. 3, where less than 5% error is observed.

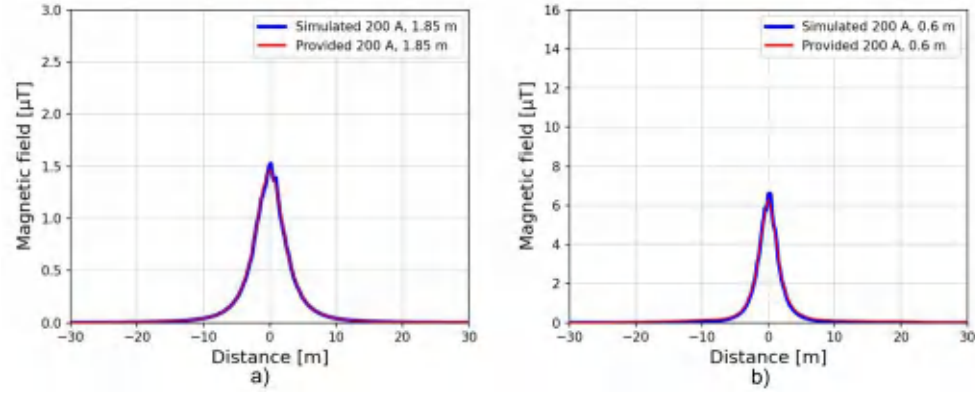

Figure 3: *Comparison between simulated and published results (in [3], Fig B.10) for RMS magnetic field near double-circuit UTL at a depth of a) 1.85 m and b) 0.6 m*

3.2 Validation with simulated results

Additional validation has been performed for the 110 kV single-circuit OTL with h_g = 15 m (see Fig. 6 and Table 2) for the electric and magnetic field levels (the latter are expressed in terms of the magnetic vector potentials). The same problem has also been simulated using a full-wave electromagnetic model based on the method of moments [10]. The results provided in Fig. 4 show excellent agreement, with less than 3% difference in the calculated electric and magnetic field levels.

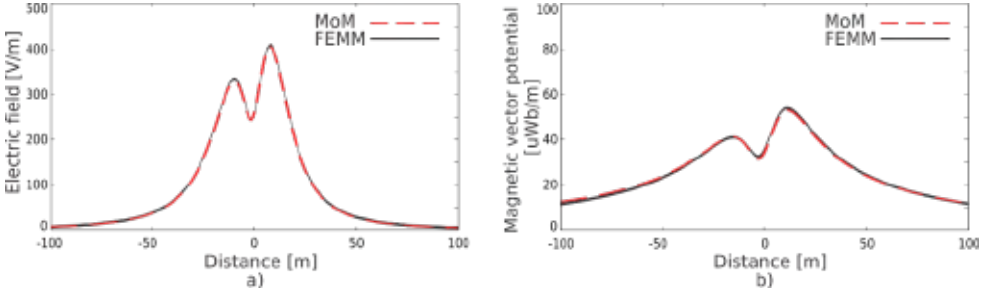

Figure 4: *Verification of the calculated RMS values of a) electric field and b) magnetic vector potential for 110 kV single-circuit transmission line with an independent MoM approach*

3.3 Validation with measurement results

The numerical results obtained in FEMM are also validated with measured values for the electric and magnetic field near OTL. The OTL in question is a 110 kV single-circuit tower with the position of the conductors provided in Table 1 (*x* values with respect to the centre of the OTL and *y* values with respect to ground level). The measurements were performed with a NARDA EFA-300 field analyser with suitable probes for electric and magnetic field measurement, and the positions provided in Table 1 were obtained by laser distance meter. When the measurements were taking place, the current strength of the conductors was nearly 100 A.

Table 1: *Position of the phase conductors and ground wire for the 110 kV single-circuit OTL*

Conductor	110 kV single-circuit	
	x [m]	*y* [m]
Phase A	3.53	7.75
Phase B	-3.07	9.55
Phase C	2.58	11.8
GW	0	17.5

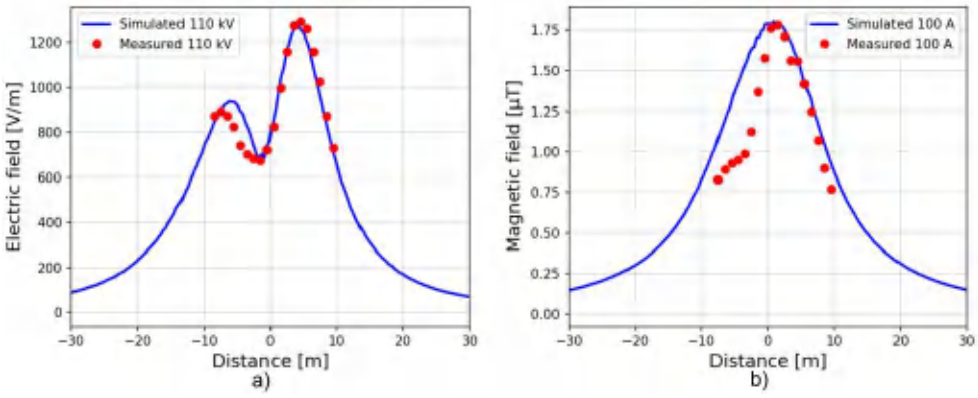

Figure 5: *Comparison between simulated and measured results for a) RMS electric field and b) RMS magnetic field for a single-circuit tower*

Fig. 5 shows the comparison between simulation and measurement results for the electric and magnetic fields at a height of 1 m from ground level, along a path perpendicular to the OTL, as required by the standard [3]. A good agreement with a 5% difference in values is mostly observed for the electric and magnetic fields, while at some points there is up to 20% difference. The error may be explained by the influence of a nearby parallel 110 kV single-circuit OTL at a distance of nearly 40 m from the analysed OTL. A better agreement of results could be expected if the contribution of the second OTL was considered.

4 PARAMETRIC ANALYSIS: RESULTS AND DISCUSSION

The subject of analysis are 110 kV single-circuit, 110 kV double-circuit, and 400 kV single-circuit overhead transmission lines. Details for the positions of the phase conductors and ground wire (GW) are provided in Fig. 6 and Table 2. The cross-sectional area of each conductor of the 110 kV OTL is 104 mm^2 (11.5 mm diameter). For the 400 kV OTL, the cross-sectional area of the phase conductors is 2 x 245 mm^2 (17.66 mm diameter each) with a mutual separation of 30 cm; for the ground wire, it is 120 mm^2 (12.36 mm diameter). Based on each conductor's previously mentioned surface area, the maximum load current for each phase conductor is 800 A and 1,920 A for the 110 kV and 400 kV towers, respectively. The parameter h_g represents the shortest distance between the conductors and the ground level. In our analysis, we consider two values of h_g: 30 m and 15 m. We assume earth with specific conductivity σ = 0.01 S/m. The electromagnetic problems have been analysed following similar procedures described in *[11]*.

Table 2: *Position of the phase conductors and ground wires for the 110 kV single-circuit, 110 kV double-circuit and 400 kV overhead transmission lines*

Conductor	110 kV single-circuit		110 kV double-circuit		400 kV single-circuit	
	x [m]	y [m]	x_1 / x_2 [m]	y [m]	x [m]	y [m]
Phase A	4.8	h_g	-3.2 / 3.2	h_g +6	-8.47	h_g
Phase B	-4.1	h_g +2.4	-3.5 / 3.5	h_g +3	0	h_g
Phase C	3.4	h_g +4.8	-3.8 / 3.8	h_g	8.47	h_g
GW	0	h_g +11	0	h_g +9	-5.07 / 5.07	h_g +4.45

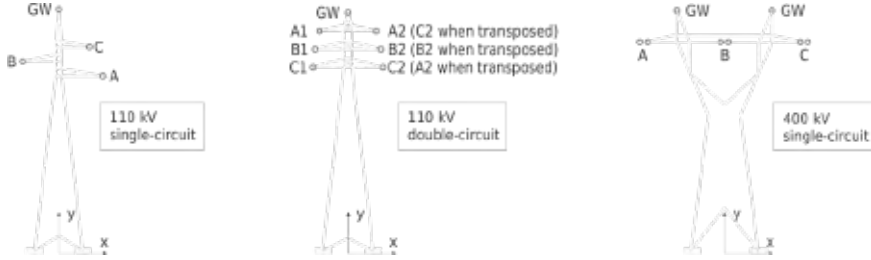

Figure 6: *Configuration of the analysed 110 kV and 400 kV overhead transmission lines*

Here we provide the simulation results for electric and magnetic fields for the different OTL configurations described in Fig. 6 and Table 2, and we compare the results with the reference levels for human exposure to electromagnetic fields provided by ICNIRP [9]. The electric and magnetic fields are computed at multiple points at a height of 1 m above ground level, along a profile perpendicular to the centre of the transmission line, as required by the standard [3]. The reference levels for general public exposure to the electric field at 50 Hz are set to 5 kV/m, and the magnetic field at the same frequency is set to 200 μT. For ground clearance of the transmission lines equal to h_g = 30 m, the results are represented by dashed lines; for h_g = 15 m, the results are represented by solid lines.

In Fig. 7, the results of the electric and magnetic fields for the single-circuit OTL are shown. It is observed that the maximum value of the electric field for the 400 kV OTL is 1.68 times lower than the reference levels, and for the 110 kV OTL, it is 12.2 times lower for the h_g = 15 m case.

In comparison, the values are further reduced by a factor of 3.54 for the h_g = 30 m case. The maximum values of the electric field appear close to the origin at x = 0 m, directly below the OTL's central axis. The 400 kV tower is an exception, where at x = 0 a sharp drop of the RMS electric field is observed mainly due to the annulment of the fields of each phase in one period. However, the range between 10 m and 20 m distance on the x-axis is of concern where the highest values of the electric field appear. Considering the system's geometry described in Table 2, this is close to the shortest distance between the ground level and the nearest phase conductor. In reality, the height of the conductors may be lower along the power line. If we consider a lower value for h_g, which is not constant along the length of the OTL, the 400 kV OTL can represent a potential risk to human health.

The maximum magnetic field value for the 400 kV OTL is 9.4 times lower, and for the 110 kV OTL it is 68 times lower than the reference levels for the h_g = 15 m case. For the h_g = 30 m case, there is a further decrease by a factor of 3.6.

Fig. 8 provides the results of the electric and magnetic fields for the double-circuit towers. The maximum values for electric and magnetic fields appear when the phases are untransposed. In the untransposed case the maximum electric field is 7.5 times lower, and in the transposed case it is 21.2 times lower than the reference levels for h_g = 15 m. In the untransposed case the maximum magnetic field is 40 times lower, and in the transposed case it is 72.9 times lower than the reference levels for h_g = 15 m. For h_g = 30 m, more than three times lower values are observed.

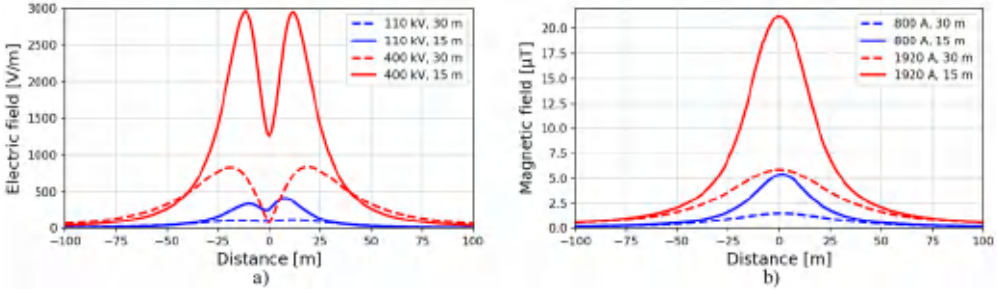

Figure 7: *a) RMS electric field and b) RMS magnetic field for single-circuit OTL*

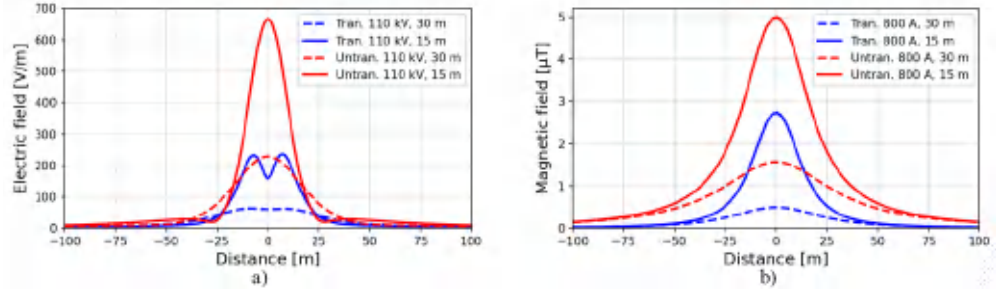

Figure 8: *a) RMS electric field and b) RMS magnetic field for double-circuit towers*

5 CONCLUSION

In this paper, we have numerically computed the RMS values of ELF electric and magnetic fields near 110 kV and 400 kV overhead transmission lines. Simulations were performed using the open-source software FEMM 4.2, using an automated procedure that has been briefly described. The electric and magnetic field levels for different OTL configurations were compared with the reference levels for human exposure to electromagnetic fields established by the ICNIRP. Additional computation and validation were done for different OTL and UTL configurations. It was observed that an error of less than 5% occurred between the computed and the reference values for validation. A comparison with measured values near an OTL was also provided, where good agreement with the computed values was observed. Therefore, in safety-related studies, the presented approach can be considered a decent substitute and an efficient method for assessing human exposure to ELF electric and magnetic fields.

Acknowledgments

This work was supported by the Ss. Cyril and Methodius University in Skopje, Project NIP. UKIM.20-21.10.

References

[1] **A. W. Wood, K. Karipidis (Eds.):** *Non-Ionizing Radiation Protection - Summary of Research and Policy Options. Part V: Extremely Low-Frequency (ELF) Electric and Magnetic Fields*, John Wiley & Sons, Hoboken, p.p. 257-338, 2017

[2] IEC TR 61000-5-1, *Electromagnetic compatibility (EMC) - Part 5-1: Installation and mitigation guidelines - General considerations*, 1996

[3] IEC 62110, *Electric and magnetic field levels generated by AC power systems - Measurement procedures with regard to public exposure*, 2009

[4] EN 50443, *Effects of electromagnetic interference on pipelines caused by high voltage a.c. electric traction systems and/or high voltage a.c. power supply systems*, 2011

[5] Directives concerning the protection of telecommunication lines against harmful effects from electric power and electrified railway systems. CCITT Directives, Vol. II, Geneva, 1989

[6] **M. V. K. Chari, S. J. Salon:** *Numerical Methods in Electromagnetism*, Academic Press, p.p. 283-357, 2000

[7] **M. N. O. Sadiku:** *Numerical Techniques in Electromagnetics*, CRC Press, Second Edition, ch. 6, 2000

[8] **M. Shabbir, M. Malik, M. Ahmad, A. Pervaiz, R. Siddique:** *Finite Element Solution for Two Dimensional Laplace Equation with Dirichlet Boundary Conditions*, Pakistan Journal of Engineering and Applied Sciences, Vol. 10, p.p. 97-102, 2012

[9] **International Commission on Non Ionizing Radiation Protection (ICNIRP):** *Guidelines for Limiting Exposure to Time-Varying Electric and Magnetic Fields (1 Hz - 100 kHz)*, Health Physics, Vol. 99, Iss. 6, p.p. 818-836, 2010

[10] **B. Markovski, L. Grcev, V. Arnautovski-Toseva:** *Fast and Accurate Transient Analysis of Large Grounding Systems in Multilayer Soil*, IEEE Transactions on Power Delivery, Vol. 36, Iss. 2, p.p. 598-606, 2021

[11] **E. Lunca, S. Vornicu, A. Salceanu, O. Bejenaru:** *2D Finite Element Model for computing the electric field strength-rms generated by overhead power lines*, Journal of Physics: Conference Series, Vol. 1065, Iss. 5, p.p. 1-4, 2018

Journal of Energy Technology

JET Volume 14 (2021)Issue 1, 2023 p.p. 51-66
Issue 1, 2023
Type of article: 1.01
http://www.fe.um.si/si/jet.htm

ANALYSIS OF REVITALISATION MODEL BEHAVIOUR FOR THERMAL POWER PLANTS IN DIFFERENT GEOGRAPHICAL AREAS

ANALIZA ODZIVANJA REVITALIZACIJSKEGA MODELA TERMOENERGETSKA POSTROJENJA NA RAZLIČNIH GEOGRAFSKIH LOKACIJAH

Martin Bricl ℜ, Jurij Avsec[1]

Keywords: revitalisation model, solar tower, heliostat field, solar irradiance, geographical location

Abstract

The implementation of renewable sources for electricity production into the energy portfolio of European countries has been a priority in recent years, especially taking into account the current geo-political changes. Even though coal is the fuel of the past, its use cannot be put aside that easily; firstly, because of the high fluctuation of electricity production from renewable sources, and secondly because of the possible negative economic impact on the economy resulting from a change in electricity prices when exiting coal. Based on the Rankine process, the authors of this paper designed a solar tower installation with a heliostat field, which enables electricity production based on solar irradiation. This combination also foresees an additional installation for flue gas desulphurisation. This combination of three processes is named the 'revitalisation model' for thermal power plants (TPPs). Based on the computer model and energy market parameters, the authors tested the 'revitalisation model' for pessimistic and optimistic scenarios. In the scope of the paper, the authors analyse the performance of the proposed 'revitalisation model' for three different

ℜ Corresponding author: Martin Bricl, Rudis d.o.o. Trbovlje, Trg revolucije 25b 1420 Trbovlje, Tel: +386 3 56 12 409, E-mail address: martin.bricl@rudis.si

1 University of Maribor, Faculty of Energy Technology, Hočevarjev trg 1, SI-8270 Krško, Slovenia

geographical locations – Berlin in Germany, Wuwei in China, and Hyderabad in India. The results of the analysis are described and shown graphically.

Povzetek

Uvajanje obnovljivih virov za proizvodnjo električne energije v energetski portfelj evropskih držav je v zadnjih letih postala prednostna naloga, še posebej zaradi spreminjajočih se geopolitičnih razmer. Premog je gorivo preteklosti, vendar ga ne moremo tako zlahka opustiti. Vodila razloga za to sta veliko nihanje proizvodnje električne energije iz obnovljivih virov in negativni ekonomski vpliv na gospodarstvo, ki bi ga lahko povzročila sprememba cen električne energije s prenehanjem uporabe premoga. Zraven obstoječega procesa Rankine smo zasnovali instalacijo solarnega stolpa s heliostatskim poljem, ki omogoča proizvodnjo električne energije na osnovi sončnega obsevanja. V tej kombinaciji smo tudi predvideli dodatno napravo za razžveplanje dimnih plinov. Ta tri-fazni proces smo poimenovali revitalizacijski model termoenergetskih postrojenj. Na podlagi računalniškega modela in parametrov energetskega trga smo preizkusili model revitalizacije za pesimistični in optimistični scenarij. V članku bomo analizirali uspešnost predlaganega modela revitalizacije za tri različne geografske lokacije – Berlin v Nemčiji, Wuwei na Kitajskem in Hyderabad v Indiji – ter prikazali rezultate analize v pisni in grafični obliki.

1 INTRODUCTION

The proposed 'revitalisation model' comprises three main elements that make up the entire proposed plant. The first component is the Rankine process [1], which represents an existing thermal power plant and has a certain operational energy and exergy efficiency in the process [2]. Coal is the primary fuel of the Rankine process (or steam process). The combustion of coal in a steam boiler releases heat, which generates steam, which is fed into a steam turbine where a shaft drives a generator for electricity production. The second component is the solar power plant, which consists of a solar tower on which the concentrated sunbeam receiver is located, and a field in which heliostatic mirrors are arranged to direct the sun's rays to a common point on the concentrated sunbeam receiver [3-5]. All the absorbed solar energy is concentrated at a certain point, thus obtaining a high temperature and consequently a high concentration of energy at a point on the solar radiation receiver. The working medium in a solar tower plant is a salt solution, which can be heated to a higher temperature than the evaporation temperature of the water. This energy (heat) is used in the evaporator to produce steam, which is conducted from the solar process back to the steam process [6]. This reduces the amount of steam that the steam boiler needs to produce to be able to run the high-pressure and low-pressure steam turbines, which rotate the generator shaft to produce electricity. This enables the energy of solar radiation [7-8] to be used to produce steam, and the load of the steam boiler in the production of steam during solar radiation can be reduced proportionally [9-13] by the amount of steam that can be produced from the solar process. Due to the lower load and production of steam from the steam boiler, the consumption of coal – a fossil fuel – is also reduced, which also reduces the required amount of carbon emission coupons, as the amount of flue gases and greenhouse gas emissions is lower at the lower load of the steam boiler in the steam process.

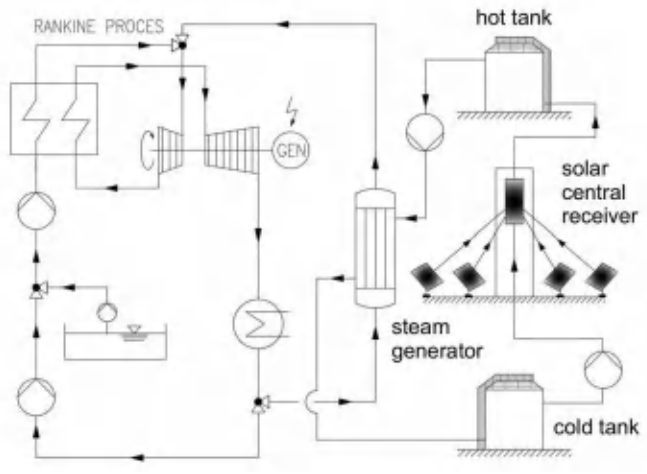

Figure 1: *The proposed 'revitalisation model' combines the traditional Rankine cycle with a solar central receiver system*

The third component of the proposed model of the revitalisation of TPPs is a plant for flue gas cleaning using the wet calcite process, which is most often identified as the best solution based on the guidelines for selecting the best possible technology. The purpose of the plant is primarily to reduce the acidic components in the flue gases and consequently reduce the impact on the environment and living beings. The advantage of the wet process is the cheap and easily accessible reagent as well as the integrity for the environment of the flue gas cleaning by-product and the specimen in it. Properly designed desulphurisation technology can achieve both high levels of purification of acidic components – sulphur dioxide as well as other air pollutants such as dust and some heavy metals [14-15]. As a by-product of flue gas cleaning, gypsum is formed, which can be used for commercial purposes (possible purchase from cement plants and gypsum board manufacturers), or it can be used to stabilise fly ash from the bottom of the steam boiler.

2 OPTIMISTIC AND PESSIMISTIC OPERATION SCENARIOS FOR THE CHOSEN GEOGRAPHICAL LOCATIONS

2.1 Geographical location Velenje, Slovenia

Figure 2, shown below, illustrates the economic performance of the proposed model. As can be seen, with the help of solar energy [16-18], the proposed model is profitable when taking into consideration the optimistic scenario, which covers all the costs of fossil fuels, the flue gas cleaning process, infrastructure maintenance and other regular maintenance costs. In this case, the proposed model would still generate EUR 1,075,400.00 in annual profit. In the figure below, the optimistic scenario is represented by the deletion-related dots and the corresponding right y-axis. The sum of monthly net profits from electricity sales is the annual economic result of the considered scenario.

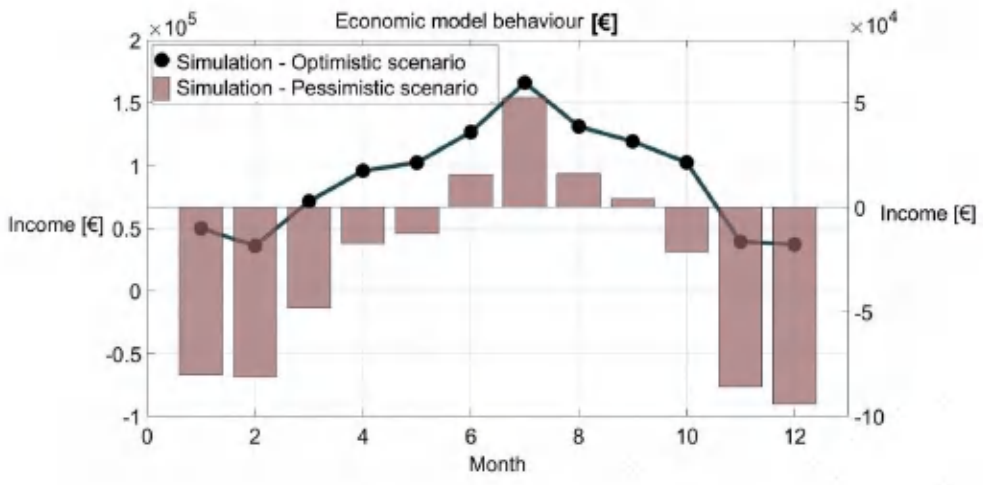

Figure 2: *Economic behaviour of the proposed 'revitalisation model' for the geographical location of Velenje, Slovenia*

Taking into account the pessimistic scenario, the costs of allowances for CO_2 emissions must be added to all the aforementioned costs, as they are a form of taxation for the operation of TPPs. In the case of the pessimistic scenario, assuming that the price of CO_2 emission allowances is expected to be higher with each additional year that a TPP operates, the model would generate EUR 353,050.00 in losses per year. This is not a bad achievement, as, without a central solar tower system, the annual loss of a TPP would be even greater.

As illustrated in Figure 2, the pessimistic scenario is shown with columns and the corresponding left y-axis. The sum of monthly net profits from electricity sales is the annual economic result of the pessimistic scenario under consideration. The proposed model and its economic benefits will play an important role in the transition from conventional fossil fuels to renewable energy sources (RES), as it would allow the simultaneous production of electricity from thermal power and renewable sources – a central solar power plant, thus maintaining a stable electricity distribution network and reducing the consumption of, and dependence on, fossil fuels.

2.2 Geographical location Wuwei, China

For the location of the city of Wuwei, China, effective solar irradiance is shown in Figure 3. Figure 4 illustrates the pessimistic and optimistic scenarios for the chosen location. Table 1 represents the income per corresponding month for the optimistic and pessimistic scenarios.

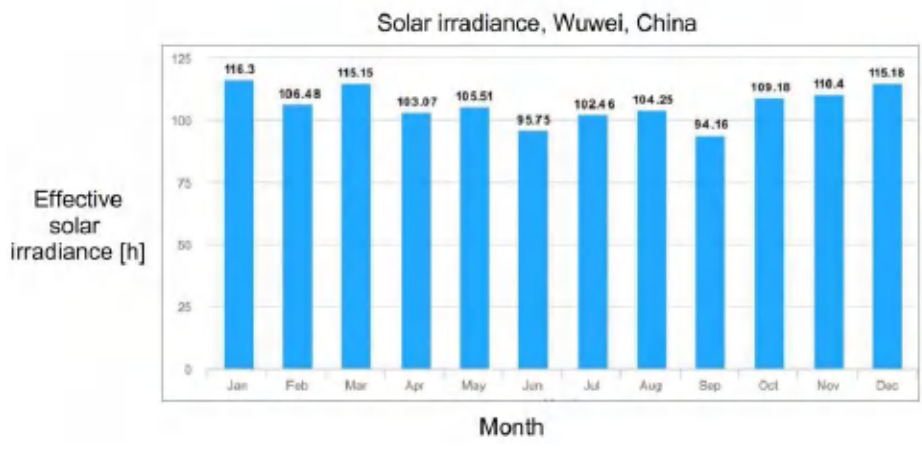

Figure 3: *Effective solar irradiance by month for the geographical location of Wuwei, China [19]*

In Figure 3, it can be seen that the effective sun irradiance expressed in hours per month is equally spread across the whole year. In Figure 4, where the realisation of the model is presented (pessimistic and optimistic scenarios) the operation of the model in the summer months is not that promising, due to the regular monsoon periods during the summer months.

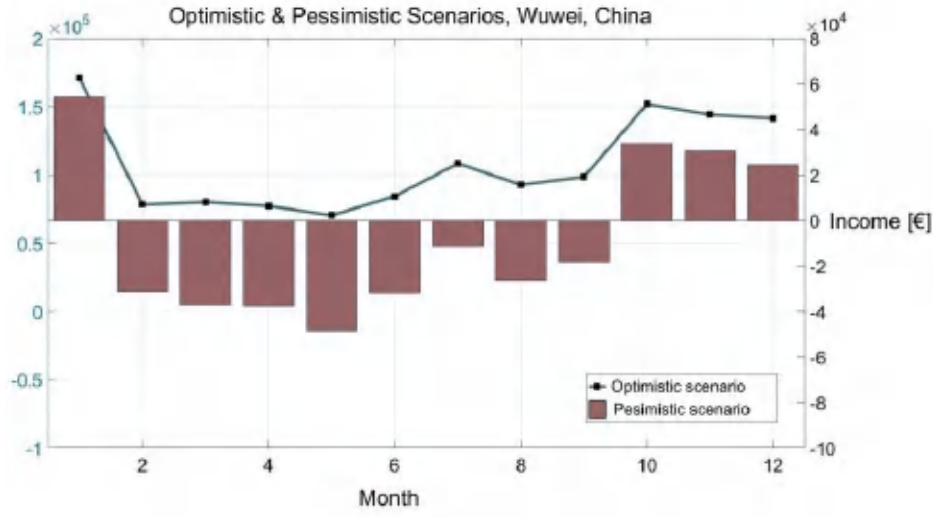

Figure 4: *Economic behaviour of the proposed 'revitalisation model' for the geographical location of Wuwei, China*

Table 1: *Economic values of model operation for an individual month in the case of optimistic or pessimistic scenarios*

Month	Optimistic scenario [€]	Pessimistic scenario [€]
January	171,020.00	54,138.00
February	78,180.00	-31,591.00
March	80,020.00	-37,073.00
April	77,160.00	-37,709.00
May	70,310.00	-48,579.00
June	84,280.00	-31,960.00
July	108,230.00	-11,227.00
August	92,710.00	-26,416.00
September	98,430.00	-18,101.00
October	151,820.00	33,619.00
November	140,403.00	30,524.00
December	141,340.00	24,256.00
TOTAL:	**1,293,903.00**	-100,119.00

2.3 Geographical location Berlin, Germany

For the location of the city of Berlin, Germany, effective solar irradiance is shown in Figure 5. Figure 6 illustrates the pessimistic and optimistic scenarios for the chosen location. Table 2 shows the income per corresponding month for the optimistic and pessimistic scenarios.

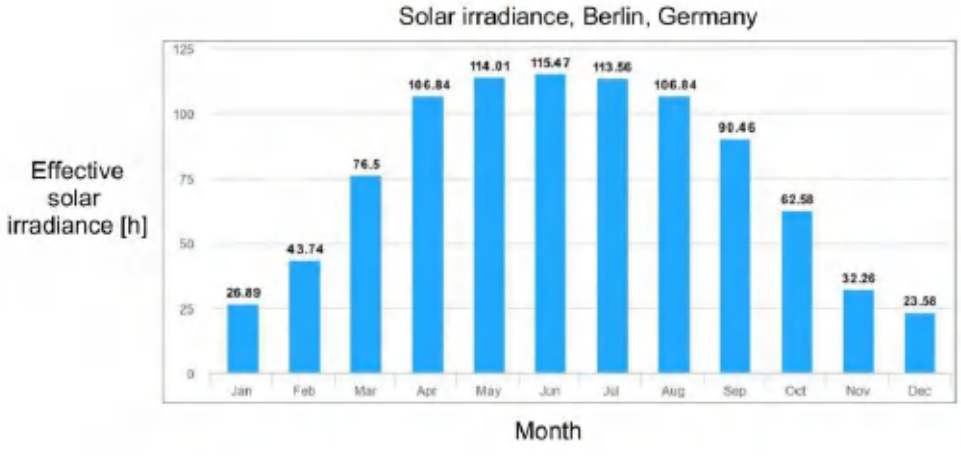

Figure 5: *Display of the time of effective solar radiation for the city of Berlin, Germany [20]*

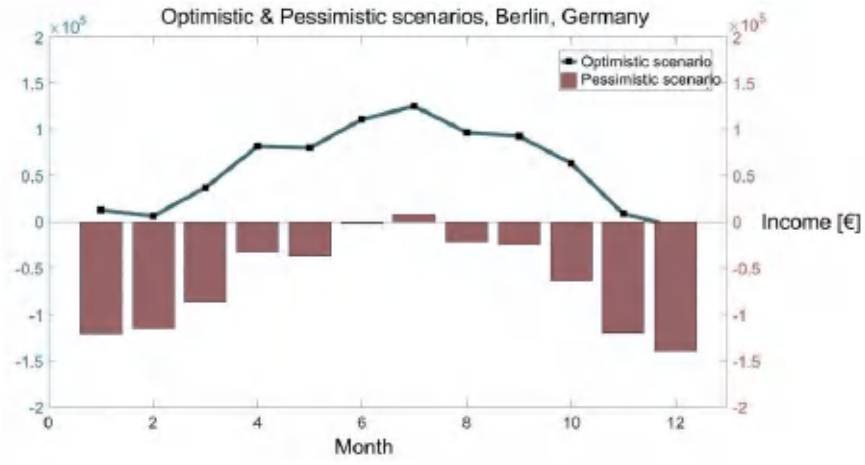

Figure 6: *Optimistic and pessimistic operating scenarios for the city of Berlin*

Table 2: *Economic values of model operation for an individual month in the case of optimistic or pessimistic scenarios*

Month	Optimistic scenario [€]	Pessimistic scenario [€]
January	12,650.00	-120,500.00
February	6,100.00	-115,350.00
March	36,780.00	-87,510.00
April	81,600.00	-32,580.00
May	79,940.00	-37,360.00
June	110,730.00	-1,840.00
July	125,020.00	7,630.00
August	96,470.00	-20,220.00
September	92,610.00	-24,610.00
October	63,230.00	-63,650.00
November	8,570.00	-119,490.00
December	-5,490.00	-139,640.00
TOTAL:	**708,210.00**	-755,120.00

2.4 Geographical location Hyderabad, India

For the location of the city of Hyderabad, India, effective solar irradiance is shown in Figure 7. Figure 8 illustrates the pessimistic and optimistic scenarios for the chosen location. Table 3 represents the income per corresponding month for the optimistic and pessimistic scenarios.

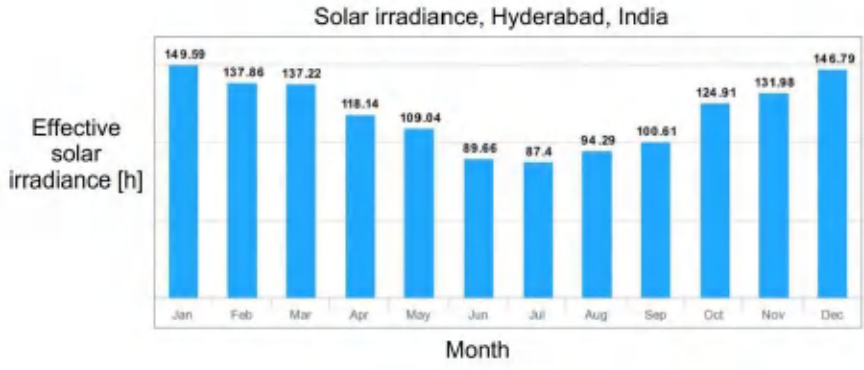

Figure 7: *Display of the time of effective solar radiation for the city of Hyderabad, India [21]*

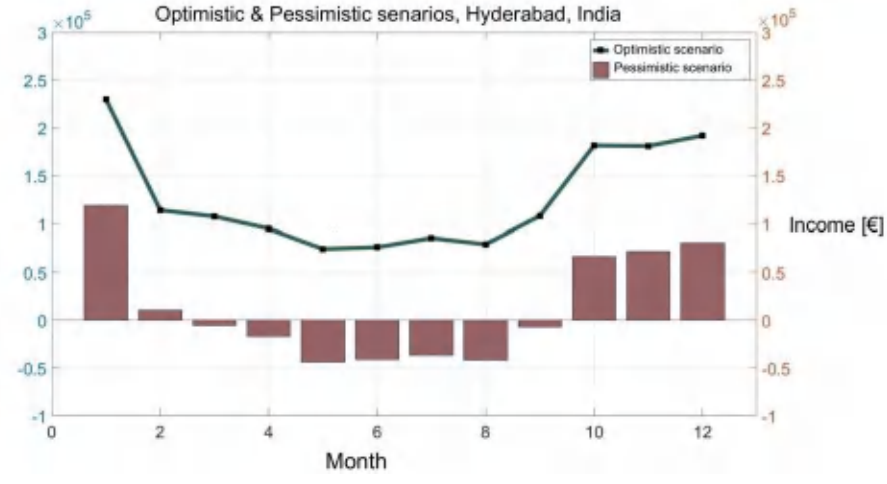

Figure 8: *Optimistic and pessimistic operating scenario of the model for the Hyderabad site*

Table 3: *Economic values of model operation for an individual month in the case of optimistic or pessimistic scenarios*

Month	Optimistic scenario [€]	Pessimistic scenario [€]
January	230,010.00	119,330.00
February	114,300.00	10,380.00
March	107,820.00	-5,170.00
April	95,180.00	-16,890.00
May	74,370.00	-43,860.00
June	76,250.00	-41,120.00
July	85,690.00	-36,570.00

August	79,260.00	-41,720.00
September	108,340.00	-6,990.00
October	181,880.00	66,610.00
November	181,270.00	71,178.00
December	192,150.00	80,940.00
TOTAL:	**1,526,520.00**	156,118.00

3 REVITALISATION MODEL RESPONSE FOR CHANGED MARKET PARAMETERS

The designed model was further analysed by considering the following parameters for the geographical location of the cities of Berlin, Hyderabad and Wuwei:

- number of hours of effective solar radiation
- local coal price
- the price of electricity for the country in which the selected geographical location is located
- the price of carbon dioxide emissions if such a taxation scheme is located in the country of the selected geographical location

3.1 Geographical location Wuwei, China

For the geographical location of Wuwei, China, when analysing the behaviour of the model, the authors considered the change in parameters that depend on local regulations and limits, as shown in Table 4.

Table 4: *Display of considered changed parameters for the location of Wuwei, China*

Parameter	Quantity	Unit
Coal price	**60.00**	[€ / t]
CO_2 emission coupon price	**/**	[€ / t]
Salaries	**9.50**	[€ / h]
Electricity price	**82.00**	[€ / MWh]

Figure 9 and Table 5 show the graphically and numerically expected realisation of the considered model for the selected location of Wuwei.

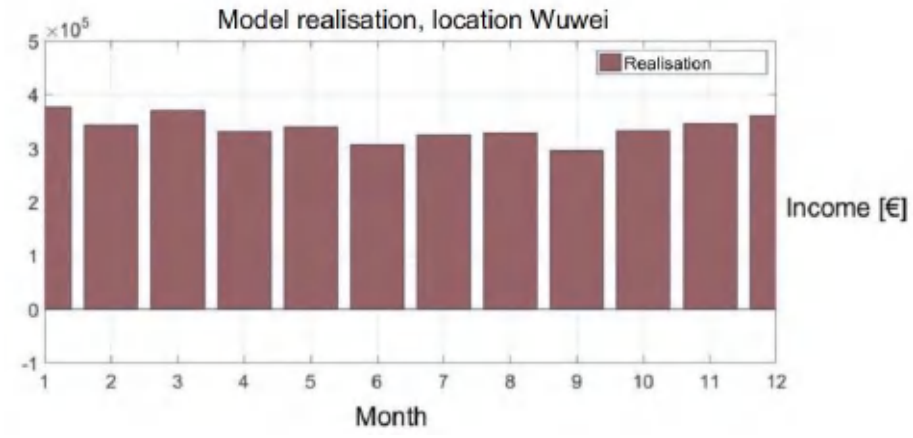

***Figure 9**: Display of the expected realisation of the model based on the changed entry parameters for the location of Wuwei*

***Table 5**: Numerical representation of the expected realisation of the realistic scenario according to the changed entry parameters for the location of Wuwei*

Month	Realistic scenario [€]
January	375,650.00
February	343,480.00
March	370,990.00
April	332,130.00
May	339,600.00
June	307,160.00
July	325,540.00
August	329,490.00
September	294,720.00
October	332,680.00
November	346,000.00
December	360,770.00
TOTAL	4,058,210.00

3.2 Geographical location Berlin, Germany

For the geographical location of Berlin, the analysis of the model behaviour took into account the change in parameters that depend on local regulations and limits, as shown in Table 6.

***Table 6**: Display of considered changed parameters for Berlin, Germany*

Parameter	Quantity	Unit
Coal price	**51.00 – 85.00**	[€ / t]
CO_2 emission coupon price	**25.00**	[€ / t]
Salaries	**30.00**	[€ / h]
Electricity price	**120.00**	[€ / MWh]

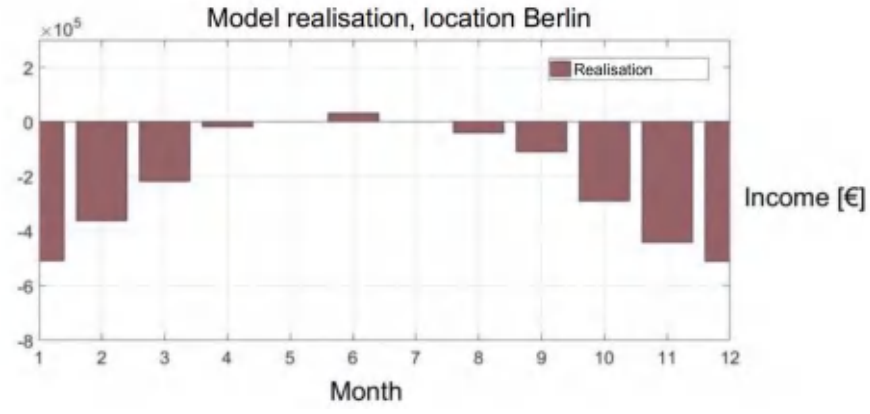

***Figure 10**: Illustration of the expected realisation of the model with changed input parameters for the location of Berlin*

***Table 7:** Numerical representation of the expected realisation of the realistic scenario according to the changed entry parameters for the location of Berlin*

Month	Realistic scenario [€]
January	-507,000.00
February	-362,090.00
March	-217,830.00
April	-19,180.00
May	320.00
June	31,700.00
July	530.00
August	-39,210.00
September	-110,040.00
October	-289,830.00
November	-441,730.00
December	-510,920.00
TOTAL	-2.465,280.00

3.3 Geographical location Hyderabad, India

For the geographical location of Hyderabad, the analysis of model behaviour took into account the change in parameters that depend on local regulations and constraints, as shown in Table 8.

Table 8: Display of considered changed parameters for Hyderabad, India

Parameter	Quantity	Unit
Coal price	**70.00**	[€ / t]
CO_2 emission coupon price	**/**	[€ / t]
Salaries	**8,35**	[€ / h]
Electricity price	**95.00**	[€ / MWh]

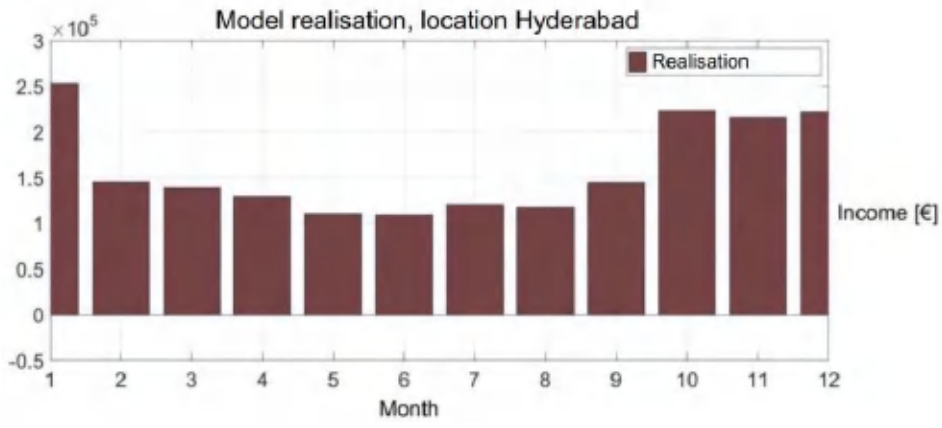

***Figure 11**: Illustration of the expected realisation of the model with changed input parameters for the location of Hyderabad*

Table 9: *Numerical representation of the expected realisation of the realistic scenario according to the changed entry parameters for the location of Hyderabad*

Month	Realistic scenario [€]
January	252,980.00
February	145,090.00
March	139,520.00
April	128,810.00
May	110,130.00
June	108,970.00
July	120,440.00
August	117,770.00
September	144,400.00
October	223,240.00
November	215,090.00
December	221,840.00
TOTAL	**1,928,280.00**

3 CONCLUSION

Table 10 summarises the results of the considered model for different geographical locations and parameters. The results for two different cases are summarised and shown for three additional locations – Wuwei, Berlin and Hyderabad,. The first example takes into account the change of geographical location only and the consequent change of hours of effective solar radiation. The second example involves changing several parameters. In addition to changes in geographical location, local fuel (coal) prices, local electricity prices, and local labour or personnel prices are also taken into account. When analysing the operation of the plant, it was found that due to high fuel costs, the production of electricity exclusively from steam generated by a steam boiler is unprofitable. Thus, the contribution of the central receiver system (CRS) is essential for the cost-effective operation of the assumed model. As demonstrated by the positive operating scenario, the proposed system would achieve positive market results in the current market situation. In the case of the pessimistic scenario, the system would only operate profitably for four months a year, which is a low amount, however, it should be noted that most TPPs operate at a loss and the state provides financial assistance for uninterrupted electricity production. The pessimistic scenario shows a positive impact of upgrading the CRS system, as the loss at the annual level of operations is reduced almost 10-fold.

Table 10: *Results of the considered model for different geographical locations and parameters*

PARAMETER	Location						
	Velenje	Wuwei		Berlin		Hyderabad	
		①	②	①	②	①	②
Effective sun irradiance [h]	1,112.3	1,267.9	1.267,9	912.7	912.7	1,427.5	1,427.5
Coal savings [t]	25,227	28,984	28.982	20,742	20.701	32,377	32,375
Amount of emitted CO2 [t]	266,508	260,000	260.757	273,300	273.441	255,500	255,538
Amount of cleaned SO2 [t]	111.8	109	109,3	114	114.6	107	107.2
Optimistic scenario [mio €]	**1.07**	**1.29**	**4,05**	**0.71**	**-2.46**	**1.52**	**1.92**
Pessimistic scenario [mio €]	**-0.35**	**-0.10**	/	**-0.75**	/	**0.15**	/

*① - Results of the considered model at the changed geographical locations (number of hours of effective solar radiation)

*② - The results of the considered model with the following parameters changed:

- Number of hours of effective solar radiation
- Consideration of the local coal price
- Observance of the local electricity price
- Taking into account the local price of labour or employees

The model represents a possible upgrade and modernisation of conventional TPPs to ensure an uninterrupted supply of electricity even in the event of an increased disruption in the thermal power system due to the production of electricity from renewable sources. Rising fossil fuel prices, and limiting them, will increase interest in the implementation of the model described and similar solutions.

References

[1] **J. Oman:** *Generatorji toplote*, Univerza v Ljubljani, Fakulteta za strojništvo, Ljubljana 2005

[2] **M. Tuma**: *Energetski sistemi: preskrba z električno energijo in toploto*, 3. izdaja; Ljubljana, Fakulteta za strojništvo, 2004

[3] **C. Baliff, D. Favrat, V. Aga, M. Romero, A. Steinfeld:** *Germain Augsburger – Thermo-economic optimisation of large solar tower power plants*, Ecole Politehique Federale De Lausanne, Suisse 2013

[4] **S. Doruk, T. Murat, O. Taylan:** *Investment Analysis of a New Solar Power Plant*, International Journal of Renewable and Sustainable Energy, Vol.2, No.6, 2013, Pages 229–241

[5] **B. Burger:** *Fraunhofer institute for solar energy systems - Electricity production from solar and wind in Germany in 2014*, Freiburg, 29 December 2014

[6] **P.S. Nolan:** *Babcock & Wilcox Company - Emission Control Technologies for Coal-Fired Power Plants*, Ministry of Electric Power Seminar; Beijing China, 1996

[7] **R. Soltani, P. Mohammadzadeh Keleshtery, M. Vahdaty, M. Rahbar, M. Amidpour:** *Theoretical utilization of high temperature solar power tower technology in a 30 MW cogeneration cycle*, Journal of Clean Energy Technologies, Vol.1, 2013

[8] **D. E. Chelghoum, A. Bejan:** *Second-law analysis of solar collectors with energy storage capability*, Transactions of ASME, Vol.107, August 1985, Pages 244–251

[9] **O. Bahar, A. Khellaf, K. Mohammedi:** *A review of studies on central receiver solar thermal power plants. Renewable and Sustainable Energy Reviews*, Vol.23, 2013, Pages 12–39

[10] **H. L. Zhang, J. Baeyens, J. Degreve, G. Caceres:** *Concentrated solar power plants: Review and design methodology*, Renewable and Sustainable Energy Reviews, Vol.22, 2013, Pages 466–481

[11] **P. A. Curto, G. Stern:** *Central solar receivers – applications for utilities and industry*, Mechanical Engineering, Vol.104, No.7, 1982

[12] **J. Sanz-Bermejo, V. Gallarado-Natividad, J. Gonzales-Aguilar, M. Romero:** *Comparative system performance analysis of direct steam generation central receiver solar thermal power plants in megawatt range*, Journal of Solar Energy Engineering, Vol.136, 2014, (9 pages)

[13] **S. C. Ksushik, V. Reddy Siva, S.K. Tyagi:** *Energy and exergy analyses of thermal power plants – a review*, Renewable and sustainable energy reviews, December 2010

[14] **H.R. Kulkarni, P.P. Revankar, S.G. Hadagal:** *Energy and exergy analysis of coal-fired power plant*, International Journal of Innovative Science and Research Technology, Vol.1, No.3

[15] **Babcock & Wilcox Company:** *Steam its generation and use*, Edition 41; Ohio, U.S.A., 1992

[16] **L. Chao, Z. Rongrong:** *Thermal performance of different integration schemes for a solar tower aided coal-fired power system*, Energy Conversion and Management, Vol.171, 2018, Pages 1237–1245

[17] **E. Spayde, P. Mango:** *Evaluation of a solar-powered organic Rankine cycle using dry organic working fluids*, Cogent Engineering, Vol.2, 2015 – Issue 1

[18] Povprečno trajanje sončnega obsevanja. (n.d.). V *Meteo.* Pridobljeno s **www.meteo.si**

[19] Efektivno sončno obsevanje za mesto Wuwei. (n.d.). V *Photovoltaic geographical information system*. Pridobljeno s **https://re.jrc.ec.europa.eu/pvg_tools/en/#MR**

[20] Efektivno sončno obsevanje za mesto Berlin. (n.d.). V *Photovoltaic geographical information system*. Pridobljeno s **https://re.jrc.ec.europa.eu/pvg_tools/en/#MR**

[21] Efektivno sončno obsevanje za mesto Hyderabad. (n.d.). V *Photovoltaic geographical information system*. Pridobljeno s **https://re.jrc.ec.europa.eu/pvg_tools/en/#MR**

Nomenclature

(Symbols)	(Symbol meaning)
t	time
h	hour
CO_2	carbon dioxide
SO_2	sulphur dioxide
€	euros
mio	million
GEN	generator
MWh	megawatt hour

Journal of Energy Technology

JET Volume 16 (2023) p.p. 67-77
Issue 1, 2023
Type of article: 1.04
http://www.fe.um.si/si/jet.htm

DESIGN OF WFOIL 18 ALBATROSS WITH HYDROGEN TECHNOLOGIES

ZASNOVA PLOVILA WFOIL 18 ALBATROSS Z VODIKOVIMI TEHNOLOGIJAMI

Nejc Zore[1ℜ], Jurij Avsec [1], Urška Novosel [1]

Keywords: wFoil 18 Albatross, hydrofoil, fuel cell drive, hydrogen technology

Abstract

This article discusses the design of fuel cell propulsion for 18 albatross foil vessels. The purpose of this article determined the economic viability of such propulsion. WFoil 18 Albatross was chosen for a high-speed, low-power propulsion system.

The hydrogen propulsion system for the Albatross vessel consists of the following parts:

- Electric motor (Emrax 188) to convert electricity into mechanical energy;
- Battery (LG RESU 3.2EX | LG Battery System), which provides electricity in case of emergency or adds the necessary energy to run the engine at maximum power;
- Controller (EmDrive 500), which provides enough energy to pass between the elements of the propulsion system;
- Fuel cell (Hydrogenics HYPM-HD 30 POWER MODULE), which is the primary source of energy;
- The tank (tank for hydrogen gas type 3) stores fuel, which in our case is hydrogen.

ℜ Corresponding author: Nejc Zore, University of Maribor, Faculty of Energy Tehnology, Hočevarjev trg 1 SI-8270, Krško, E-mail address: nejczore20@gmail.com

1 University of Maribor, Faculty of Energy Tehnology, Hočevarjev trg 1 SI-8270, Krško, Slovenia

The brackets indicate the parts that have been selected for the hydrogen propulsion system. The approximate weight of all these parts is about 249.1 kg and the price of all these parts is about 55254 €. All prices are from 2020 and are subject to change.

The main idea in the construction of this charging station is the use of seawater and solar energy or renewable energy sources for hydrogen production. The components of the charging station are Solar cells (LG NeON 2), Desalination (CRYSTAL EX PURE), Electrolysis (Nel C Series C10), and Charging station (Haskel (Version with air compressor)).

The brackets indicate the parts that have been selected for the charging station. The approximate weight of all these parts is about 10236 kg and the price of all these parts is about 517664 €. All prices are from 2020 and are subject to change.

Povzetek

Ta članek obravnava zasnovo pogona na gorivne celice za 18 plovil albatrosa. Namen tega članka je določil ekonomsko upravičenost takšnega pogona. WFoil 18 Albatross je bil izbran za pogonski sistem visoke hitrosti in nizke moči.

Pogonski sistem na vodik za plovilo Albatros je sestavljen iz naslednjih delov:

- Elektromotor (Emrax 188) za pretvorbo električne energije v mehansko;
- Baterija (LG RESU 3.2EX | LG Battery System), ki zagotavlja elektriko v nujnih primerih ali doda potrebno energijo za delovanje motorja z največjo močjo;
- Krmilnik (EmDrive 500), ki zagotavlja dovolj energije za prehajanje med elementi pogonskega sistema;
- Gorivna celica (Hydrogenics HYPM-HD 30 POWER MODULE), ki je primarni vir energije;
- Rezervoar (rezervoar za plin vodik tip 3) hrani gorivo, ki je v našem primeru vodik.

Oklepaji označujejo dele, ki so bili izbrani za pogonski sistem na vodik. Približna teža vseh teh delov je približno 249,1 kg, cena vseh teh delov pa je približno 55254 €. Vse cene so od leta 2020 in se lahko spremenijo.

Glavna ideja pri izgradnji te polnilnice je uporaba morske vode in sončne energije oziroma obnovljivih virov energije za proizvodnjo vodika. Sestavni deli polnilne postaje so sončne celice (LG NeON 2), razsoljevanje (CRYSTAL EX PURE), elektroliza (Nel C serije C10) in polnilna postaja (Haskel (različica z zračnim kompresorjem)).

Oklepaji označujejo dele, ki so bili izbrani za polnilno postajo. Približna teža vseh teh delov je približno 10236 kg, cena vseh teh delov pa je približno 517664 €. Vse cene so od leta 2020 in se lahko spremenijo.

1 INTRODUCTION

1.1 Platform

The basis of the platform is a trimaran to which four hydrofoils are attached: the main or rear pair of hydrofoils and the front or stabilizer pair of hydrofoils, as shown in Figure 1.

In principle, we can say that all four hydrofoils determine the whole, since they only work stably around the longitudinal and transverse axes of movement. The vessel maintains its position along these two directions and requires only vertical rudder to maintain course.

Figure 1: *Distribution of hydrogen propulsion elements throughout the vessel*

In addition to stability, the double "V" arrangement of hydrofoils has an advantage over classic vessels by enabling both calm sailing in rough, wavy seas and (due to the folding system, otherwise relatively long hydrofoils) the possibility of sailing in very shallow seas and even landing on sandy beaches. This makes the vessel an economical, comfortable and very useful platform for various types of vessels.

When sailing at high speed, the hulls are quite high above the surface of the water, so that the waves do not affect the sailing itself. The vessel has been tested in extreme conditions and has always offered calm sailing with much less strain on its structure. Figure 2 shows two different graphs of water resistance and speed for two different concepts, namely for the constantly wetted system and for the wFoil system.

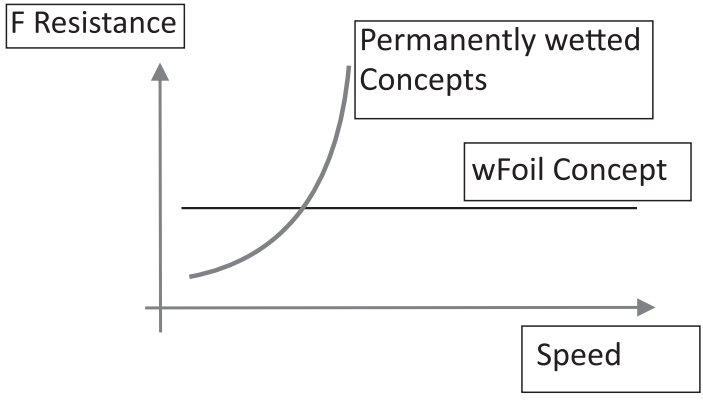

Figure 2: *Graph of water resistance and speed*

From the above description, we can understand that the wFoil platform offers the following properties, which are far ahead of the properties of classic vessels and also of other hydrofoil vessels:

- By increasing the sailing speed, the vessel rises above the water surface, so that the hulls of the vessel do not touch the waves. Hydrofoils are relatively long compared to the size of the vessel, which allows calm, fast, comfortable and safe navigation in rough seas.
- At higher speeds, the hydrodynamic resistance of the vessel is lower than that of other vessels - even vessels that use hydrofoils. This feature occurs because the wetted part of hydrofoils decreases with increasing sailing speed.
- wFoil vessel is also useful in very shallow waters. We can also land on sandy beaches, which is possible thanks to the unique system of folding the otherwise relatively long hydrofoils under the transverse supports of the platform structure.
- The wFoil platform, with its hydrofoil arrangement, only enables stability around the transverse and longitudinal axes of movement. This allows the vessel's platform to remain in a more or less horizontal position without the use of complicated systems to maintain stability.

1.2 Benefits

The main advantages of the wFoil platform are listed below:

- Directivity and stability of the vessel
- Smaller hydrodynamic resistance
- Greater range of useful vessel speeds
- Folding hydrofoils
- Wave compensation
- Economical construction and easy maintenance.

2. CONSTRUCTING A HYDROGEN PROPULSION

2.1 Conceptual design of a hydrogen drive

The hydrogen propulsion system for the Albatross vessel consists of parts as shown in Figure 3:

- Electric motor for converting electrical energy into mechanical energy;
- A battery that provides electricity in case of emergency or adds the necessary energy for the engine to operate at maximum power;
- A controller that provides enough energy to pass between the elements of the drive assembly;
- Fuel cell, which is the primary source of energy;
- The tank stores the fuel, which in our case is hydrogen.

Figure 4 shows the distribution of propulsion elements across the vessel.

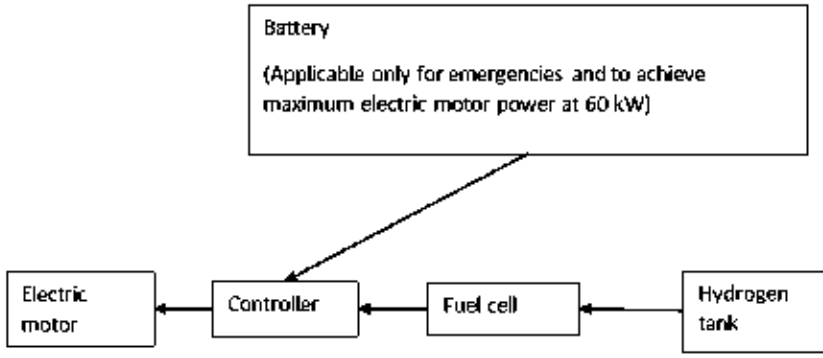

Figure 3: *Scheme of the hydrogen drive.*

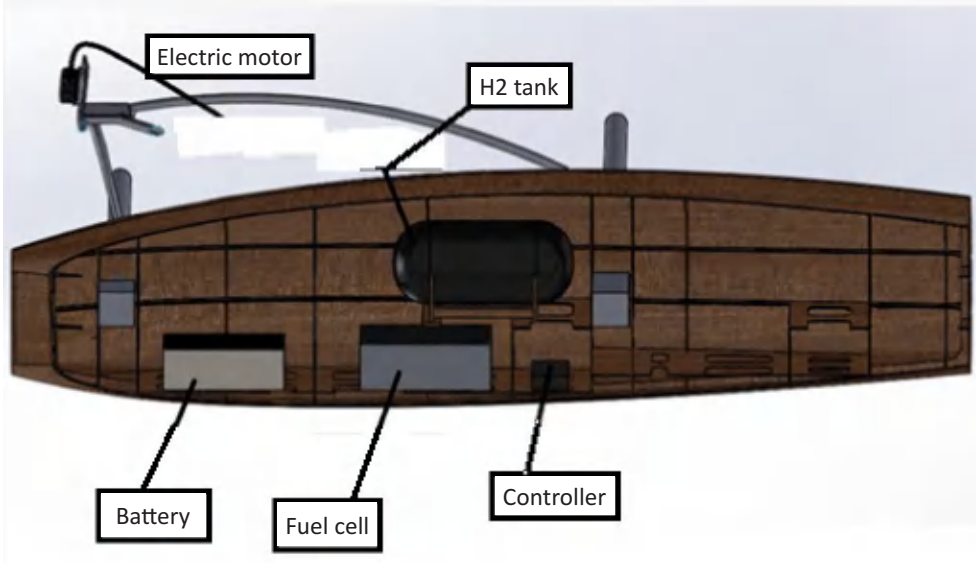

Figure 4: *Distribution of hydrogen propulsion elements throughout the vessel*

2.2 Components

Electric motor: Emrax 188
Battery: LG RESU 3.2EX | LG Battery System
Controller: EmDrive 500
Fuel cell: Hydrogenics HYPM-HD 30 POWER MODULE
Reservoir H2: Reservoir for hydrogen gas type 3

Table 1: *Hydrogen propulsion components*

	Electric motor	Controller	Fuel Cell	H2 Tank	Battery	Total
Voltage [V]	110	30 - 125	60 - 120	/	45,2 – 58,1	/
Current [A]	0 - 800	0 - 800	0 - 500	/	/	/
Dimensions [mm]	Ø 188 × 77	78 × 310 × 205	719 × 406 × 261	Ø 460 × 991	230 × 664 × 165	/
Mass [kg]	7,2	4,9	75	102	60	249,1
Efficiency [%]	96	96	53	/	85	/
Price [€]	3.700	1.900	39.000	5.090	5.564	55.254
Model	Emrax 188 (LV)	EmDrive 500	HD30	SHC 90L 700 bar	LG RESU 3.2 EX	/

2.3 Calculation for the hydrogen propulsion system

Calculation of the total weight of the hydrogen propulsion system for the Albatross

$$7{,}2\ kg + 4{,}9\ kg + 75\ kg + 102\ kg + 60\ kg = 249{,}1\ kg \tag{2.1}$$

Calculation of total efficiency for operation on fuel cells

$$0{,}96 + 0{,}96 + 0{,}53 = 0{,}488 \tag{2.2}$$

Calculation of total efficiency for battery operation

$$0{,}96 + 0{,}96 + 0{,}85 = 0{,}78 \tag{2.3}$$

Calculation of the final price of all elements in the drive

3700€ + 1900€ + 39000€ + 5090€ + 5564€ = 55254€ (2.4)

2.4 Comparison between a gasoline engine and a hydrogen engine

Figure 5 shows a comparison between gasoline engine and hydrogen drives. The figure includes the fuel for both drives, the yields and the products produced by the drives.

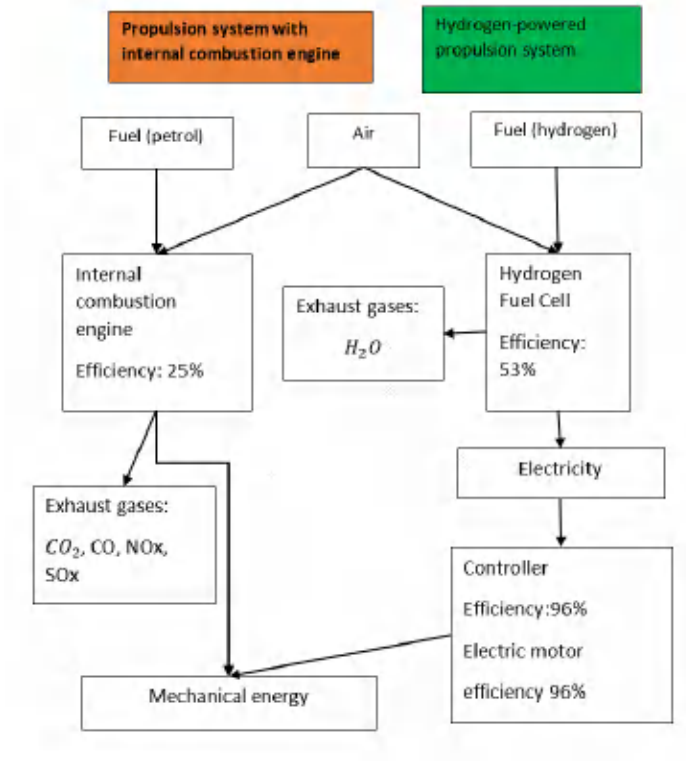

Figure 5: *Comparison of energy conversions*

Calculation for a gasoline engine:

$$0{,}75\,\frac{kg}{l} \times 25\,l = 18{,}75\,kg \tag{2.5}$$

$$12\,\frac{kWh}{kg} \times 18{,}75\,kg = 225\,kWh \tag{2.6}$$

$$225\,kWh \times 0{,}25 = 56{,}25\,kWh \tag{2.7}$$

Calculation for hydrogen propulsion:

$$33{,}33\,\frac{kWh}{kg} \times 3{,}5\,kg = 116{,}66\,kWh \tag{2.8}$$

$$116{,}66\,kWh \times 0{,}53 = 61{,}83\,kWh \tag{2.9}$$

$$61{,}83\,kWh \times 0{,}96 = 59{,}35\,kWh \tag{2.10}$$

$$59{,}35\;\;kWh \times 0{,}96 = 56{,}98\,kWh \tag{2.11}$$

3. CONSTRUCTING A HYDROGEN CHARGING STATION

3.1 Conceptual design of the charging station

The main idea in constructing this charging station is the use of seawater and solar energy or renewable energy sources for the production of hydrogen. Figures 7 and 8 show the process for obtaining and storing hydrogen. Figure 6 shows the charging station, which was made in the computer program Solidworks.

Figure 6: *Charging station*

For proper use, seawater must be desalinated. Electricity is obtained from solar cells, and in case of bad weather from the electricity grid. When water is desalinated, it goes through electrolysis, yielding hydrogen, which serves as our fuel. The next step is to increase the pressure to 700 bar and store it in a pressure vessel until the next filling.

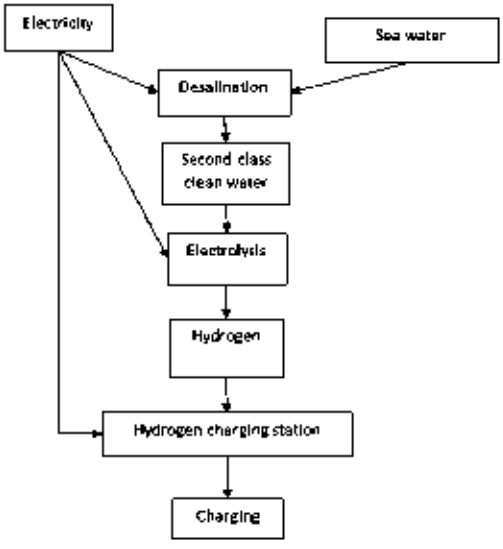

Figure 7: Scheme of the charging station

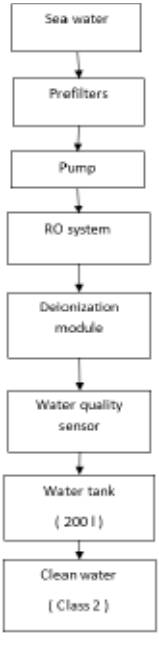

Figure 8: Sheme of the desalination proces.

3.2 Components

Solar cells: LG NeON 2
Desalination: CRYSTAL EX PURE
Electrolysis: Nel C Series C10
Charging station: Haskel (Implementation with the help of an air compressor)

Table 2: *Components of the charging station*

	Solar cells	**Desalination**	**Electrolysis**	**Charging station**	**Total**
Consumption	29,26 MWh/year	27,5 kWh/m^3	68,9 kWh/kg H2	1.680 kWh/day (max)	
Dimensions [m]	/	$0{,}4 \times 0{,}35 \times 0{,}55$	$2{,}52 \times 1{,}16 \times 2{,}01$	$3 \times 3 \times 3$	
Mass [kg]	1.386	216	2.734	6000	10.236
Product	Electricity (AC)	Clean Water (Class 2)	Hydrogen gas at 30 bar	Hydrogen gas at 700 bar	
Price [€]	30.550	3.114	240.000	244.000	517.664
Model	LG and Fronius	Crystal Ex Pure	Nel C10	Haskel air driven option	

3.3 Calculation for the charging station

Calculation of the mass of the charging station:

$$1386\ kg + 216\ kg + 2734\ kg + 6000\ kg = 10336\ kg \tag{3.1}$$

Calculation of the charging station price:

$$30550€ + 3114€ + 240000€ + 244000€ = 517664€ \tag{3.2}$$

Nominal power of the system:

$$355\ W \times 75 = 26625\ kW \tag{3.3}$$

Amount of expected annual production:

$$26625\ kW\ \times 1100\ kWh = 29288\ MWh \tag{3.4}$$

$$364€ \times 75 = 27300€ \quad (3.5)$$

Total prices of inverter and solar panels:

$$27300€ + 3234€ = 30534€ \quad (3.6)$$

How much hydrogen is produced per hour?

$$\frac{10}{22,4} = 0,45\ kmol/h \quad (3.7)$$

$$0,45 \frac{kmol}{h} \times 2 = 0,9\ kg/h \quad (3.8)$$

How much energy do we get from 1 kg of hydrogen?

$$33,33 \frac{kWh}{kg} \times 0,488 = 16,27\ kWh/kg \quad (3.9)$$

How much energy do we get from a full tank of hydrogen?

(The amount should be comparable to 25 liters of gasoline, which is enough for about 2 hours of sailing).

$$16,27 \frac{kWh}{kg} \times 3,5\ kg = 56,59\ kWh \quad (3.10)$$

How many kilograms do we need to fill the tank four times?

$$3,5\ kg\ \times 4 = 14\ kg \quad (3.11)$$

How long does it take to produce the necessary fuel?

$$\frac{14\ kg}{0,9kg/h} = 16\ h \quad (3.12)$$

How many liters of water are needed to produce fuel?

$$9 \frac{l}{h} \times 16h = 144\ l \quad (3.13)$$

How much electricity do we need for such production?

$$68,9 \frac{kWh}{kg}\ \times 14\ kg = 964,6\ kWh \quad (3.14)$$

4. CONCLUSION

The current fuel cell technology is suitable for propulsion of the wFoil 18 Albatross, but it is not economically comparable to a petrol engine.

Another drawback is the heavier weight than the internal combustion drive. Until material and production prices are reduced, hydrogen technologies will remain uncompetitive with internal combustion engines. However, they are environmentally friendly and have higher efficiencies than conventional propulsion systems.

Additional problems arise when setting up the system and obtaining appropriate approvals. To continue research for an alternative drive for the wFoil Albatross, batteries only are recommended, but this is also likely too heavy for the vessel's current limitations.

References

[1] **N. Zore:** *Zasnova plovila WFoil 18 Albatross z vodikovimi tehnologijami,* Diplomska naloga, 2020

[2] **T. Zore:** *Naprava za premikanje po vodi in/ali po zraku in/ali po kopnem*, P-200900187, 2012

[3] Gostota bencina. Fizične in kemične lastnosti. Internet archive wayback machine. Dosegljivo: https://web.archive.org/web/20020820074636/http:/www.sefsc.noaa.gov/HTMLdocs/Gasoline.htm [datum dostopa: 28.9.2022]

[4] Energetske vrednosti bencina in vodika. Idealhy.
Dosegljivo:
https://www.idealhy.eu/index.php?page=lh2_outline&fbclid=IwAR3sASHkd5P1C8wPvMDKKrU0ZAR-rDnqhn631pPoD7tJHDzdxh18zON895k [datum dostopa: 28.9.2022]

Nomenclature

(Symbols)	(Symbol meaning)
%	percent
NOx	Nitric oxide
CO2	Carbon dioxide
SOx	Sulfur oxides
CO	Carbon monoxide
H2O	water
€	euro

Journal of Energy Technology

Author instructions

http://www.fe.um.si/si/jet.htm

MAIN TITLE OF THE PAPER

SLOVENIAN TITLE

Author[1], Author [2], Corresponding author [ℜ]

Keywords: (Up to 10 keywords)

Abstract

Abstract should be up to 500 words long, with no pictures, photos, equations, tables, only text.

Povzetek

(Abstract in Slovenian language)

Submission of Manuscripts: All manuscripts must be submitted in English by e-mail to the editorial office at jet@um.si to ensure fast processing. Instructions for authors are also available online at http://www.fe.um.si/en/jet/author-instructions.html.

Preparation of manuscripts: Manuscripts must be typed in English in prescribed journal form (MS Word editor). A MS Word template is available at the Journal Home page.

A title page consists of the main title in the English and Slovenian language; the author(s) name(s) as well as the address, affiliation, E-mail address, telephone and fax numbers of author(s). Corresponding author must be indicated.

Main title: should be centred and written with capital letters (ARIAL bold 18 pt), in first paragraph in English language, in second paragraph in Slovenian language.

Key words: A list of 3 up to 6 key words is essential for indexing purposes. (CALIBRI 10pt)

[ℜ] Corresponding author: Title, Name and Surname, Organisation, Department, Address, Tel.: +XXX x xxx xxx, E-mail address: x.x@xxx.xx

[1] Organisation, Department, Address

[2] Organisation, Department, Address

Abstract: Abstract should be up to 500 words long, with no pictures, photos, equations, tables, - text only.

Povzetek: - Abstract in Slovenian language.

Main text should be structured logically in chapters, sections and sub-sections. Type of letters is Calibri, 10pt, full justified.

Units and abbreviations: Required are SI units. Abbreviations must be given in text when first mentioned.

Proofreading: The proof will be send by e-mail to the corresponding author in MS Word's Track changes function. Corresponding author is required to make their proof corrections with accepting or rejecting the tracked changes in document and answer all open comments of proof reader. The corresponding author is responsible to introduce corrections of data in the paper. The Editors are not responsible for damage or loss of submitted text. Contributors are advised to keep copies of their texts, illustrations and all other materials.

The statements, opinions and data contained in this publication are solely those of the individual authors and not of the publisher and the Editors. Neither the publisher nor the Editors can accept any legal responsibility for errors that could appear during the process.

Chapter examples:

1 MAIN CHAPTER (Arial bold, 12pt, after paragraph 6pt space)

1.1 Section (Arial bold, 11pt, after paragraph 6pt space)

1.1.1 Sub-section (Arial bold, 10pt, after paragraph 6pt space)

Example of Equation (lined 2 cm from left margin, equation number in normal brackets (section.equation number), lined right margin, paragraph space 6pt before in after line):

Equation (1.1)

Tables should have a legend that includes the title of the table at the top of the table. Each table should be cited in the text.

Table legend example:

Table 1: *Name of the table (centred, on top of the table)*

Figures and images should be labelled sequentially numbered (Arabic numbers) and cited in the text – Fig.1 or Figure 1. The legend should be below the image, picture, photo or drawing.

Figure legend example:

Figure 1: *Name of the figure (centred, on bottom of figure, photo, or drawing)*

References

[1] **N. Surname:** *Title,* Journal Title, Vol., Iss., p.p., Year of Publication

[2] **N. Surname:** *Title,* Publisher, Year of Publication

[3] **N. Surname:** *Title* [online], Publisher or Journal Title, Vol., Iss., p.p., Year of Publication. Available: website (date accessed)

Examples:

[1] **J. Usenik**: *Mathematical model of the power supply system control*, Journal of Energy Technology, Vol. 2, Iss. 3, p.p. 29 – 46, 2009

[2] **J. J. DiStefano, A.R. Stubberud, I. J. Williams**: *Theory and Problems of Feedback and Control Systems*, McGraw-Hill Book Company, 1987

[3] **T. Žagar, L. Kegel**: *Preparation of National programme for SF and RW management taking into account the possible future evolution of ERDO* [online], Journal of Energy Technology, Vol. 9, Iss. 1, p.p. 39 – 50, 2016. Available: http://www.fe.um.si/images/jet/Volume 9_Issue1/03-JET_marec_2016-PREPARATION_OF_NATIONAL.pdf (7. 10. 2016)

Example of reference-1 citation: In text *[1],* text continue.

Nomenclature

(Symbols)	(Symbol meaning)
t	time

JET

JET I Journal of Energy Technology I Vol. 16, Issue 1, Junij 2023 I University of Maribor, Faculty of Energy Technology

ISSN 1855-5748

9 771855 574008